First and Second Law Analysis of Gas Turbine and Solid Oxide Fuel Cell Hybrid System

A Major thesis submitted

In partial fulfilment of the requirements for the award of the degree of

Master of Engineering

In

Thermal Engineering

By

Bal Krishan Mishra

Roll. No. 03/THR/09

Univ. Roll No.-8573

Session 2009-11

Under the Guidance of

Dr. R.S. Mishra, Professor

Department of Mechanical Engineering

Faculty of Technology, University of Delhi

Delhi-110007, INDIA

STUDENT'S DECLARATION

I hereby certify that the work which is being presented in the minor project entitled **"Thermodynamic Modelling of Gas Turbine and Solid Oxide Fuel Cell Hybrid System"** in partial fulfilment of the requirements for the award of the degree of Master of Engineering in Thermal Engineering, submitted to the Department of Mechanical Engineering, is an authentic record of my own work carried under the supervision of **Dr. R.S. Mishra, Professor** of Mechanical Engineering Department, Faculty of Technology, University of Delhi, Delhi.

I have not submitted the matter embodied in this major project as whole or in part, for the award of any other degree.

Bal Krishan Mishra

ME (Thermal Engineering)

Univ. Roll No.-8573

CERTIFICATE

Date: _____

This is to certify that the dissertation entitled **"Thermodynamic Modelling of Gas Turbine and Solid Oxide Fuel Cell Hybrid System"** submitted by **Mr. Bal Krishan Mishra (**03/THR/09), (University Roll. No.8573) in partial fulfilment for the award of the Degree of Master of Engineering in Thermal Engineering of University of Delhi, is an authentic record of student's own work carried out by him under my guidance and supervision.

Dr. R.S. Mishra

Professor,

Department of Mechanical Engineering
Faculty of Technology

University of Delhi, Delhi

ACKNOWLEDGEMENT

It is distinct pleasure to express my deep sense of gratitude and indebtedness to my learned supervisor **Dr. R.S. Mishra, Professor** in the Department of Mechanical Engineering, Faculty of Technology, University of Delhi, Delhi, for his invaluable guidance, encouragement and patient review. His continuous inspiration only has made me complete this major project.

I am thankful to **Dr. S.S. Kachhwaha, Professor,** School of Engineering and Technology, Pandit Deendayal Petroleum University, Gandhinagar, Gujarat, for his kind support and guidance.

I am thankful to my all teachers, classmates and friends for their unconditional support and motivation during this project. It is a great opportunity for me to extend my heartiest felt gratitude to everybody who helped me throughout the course of this minor project in anyway.

Bal Krishan Mishra
ME (Thermal)
Univ. Roll. No. 8573

Table of Contents

Chapter 3

List of Tables

List of Figures

NOMENCLATURE

A_T	Total area
A_c	Cell area (cm^2)
D_{eff}	Effective diffusion coefficient
E	Neranst voltage (V)
E^o	Maximum expected voltage (V)
E^{oo}	Thermal voltage (V)
F	Faraday's constant (96,485 C/eq)
i	Current density (A/ cm^2)
i_o	Exchange current density (A/ cm^2)
i_L	Limiting current density (A/ cm^2)
I	Cell current (A)
MW	Molecular weight
n	Number of electron passed per mole of species (mole of x/s)
$\dot{n}_x$	Rate of molar consumption or production of species x (mole of x/s)
N_s	Number of stack
N_{cell}	Number of cell
N_{cell}^{stack}	Number of cell per stack
P_e	Electrical power (kW)
q	Charge passed per mole of species
R	Resistance (Ω)

R_u	Universal gas constant
T	Temperature (K)
V_s	Stack voltage (V)
V_{cell}	Cell voltage (V)
w_e	Electrical work (kW)

Greek

$\eta_{a,a}$	Activation over potential at anode (V)
$\eta_{a,c}$	Activation over potential at cathode (V)
$\eta_{c,a}$	Concentration polarization at anode (V)
$\eta_{c,c}$	Concentration polarization at cathode (V)
η_f	Fuel utilization efficiency (%)
η_R	Ohmic losses (V)
η_x	Losses due to species crossover (V)
δ	Diffusion layer thickness
σ	Conductivity
ρ	Resistivity
η_{th}	Thermodynamic cell efficiency (V)

Subscript / Superscript

AC	Alternating current
CHP	Combined heat and power

$cell$	Cell
DC	Direct current
e	Electrical
eff	Effective
GT	Gas turbine
max	Maximum
MGT	Micro gas turbine
MW	mega Watt
s	Stack
th	Thermodynamic
PSOFC	Planar solid oxide fuel cell
SOFC	Solid oxide fuel cell
SPGI	Siemens power generation Inc.
TIT	Turbine inlet temperature
TSOFC	Tubular solid oxide fuel cell

ABSTRACT

This work reports an assessment of coupling micro gas turbine and high temperature fuel cell (SOFC) as a possibility to realize power plant with an efficiency of 60% to70%. The application of such a technology will be in the decentralized feed-in of housing estates and buildings with electricity, heat and cooling energy and further can be extended to centralized power plant with the developments in the technology of commercial fuel cell. Nowadays the first implemented prototypes reach efficiencies among 57- 58%. Solid oxide fuel cell (SOFC) stacks are at the core of complex and efficient energy conversion systems for distributed power generation. Such systems are currently in various stages of development. A micro gas turbine working alone has a lower efficiency around 30%. A fuel cell is a clean energy generator but it also has lower plant efficiency when fuel cell is used alone. A hybrid system combines the micro gas turbine and fuel cell to achieve a higher efficiency around 60 -70% by utilizing the exhaust of both fuel cell and micro gas turbine. A major amount of power output of the plant is generated by the fuel cell and fraction of the plant power output is generated by the micro gas turbine. The advantage of fuel cell is that it is not a heat engine and it is not limited by the Carnot efficiency, and since the efficiency of fuel cell is not limited by the second law of thermodynamics it can be reached up to 100%.

The mathematical model developed for SOFC/GT hybrid system, the developed model is then simulated in EES software. The SOFC/GT fueled with methane as fuel, an electrical efficiency of 66.5% using first law approach based upon LHV of fuel is calculated from the simulation of the developed model and delivering 1.5 MW power. The second law efficiency is also calculated and found 63.5%.In such a system more than 70% of the total power output is contributed by the SOFC unit.

Chapter 1

Introduction

We all are very well acquainted with the law of conservation of energy i.e. energy neither can be created nor destroyed and we do agree also with the doctrine, that the sources of energy are limited. On another hand, increasing use and diminishing resources of fossil fuels and concerns about environmental issues such as emissions and global warming are leading people to pay more attention towards alternative resources of energy and highly efficient energy conversion systems.

An extensive research is in progress in the field of fuel cell-gas turbine combined power plant systems. These systems use a high temperature fuel cell and a gas turbine to achieve higher overall performance and efficiency than a single mode power plant. Due to the high temperature of the exhaust gasses of the fuel cell, heat can be recuperated and used to drive a gas turbine. The gas turbine produces additional power by expansion of the exhaust gases and hence, utilizes the heat available in the exhaust of the fuel cell.

1.1 Introduction to hybrid system

Hybrid Systems are power generation systems in which a heat engine, such as a gas turbine, is combined with a non-heat-engine, such as a fuel cell. The resulting system exhibits a synergism in which the combination performs with an efficiency that far exceeds that which can be provided by either system alone. Thus the combination performs better than the sum of its parts. The working definition of Hybrid Power Systems is evolving, but currently the following statement captures the basic elements:

Hybrid Power Systems combine two or more energy conversion devices that when integrated provide

(1) Additional advantages over those devices operated individually, and

(2) A synergism that yields performance that exceeds the sum of the components.

Based upon the definition of hybrid system, combination of gas turbine with a fuel cell (High temperature fuel cell) is a hybrid system. There are basically two methods which are generally used for coupling a micro turbine with a fuel cell to achieve a gas turbine and fuel cell hybrid system for power generation.

1. Integration of a Micro Turbine and a SOFC by a Heat Exchanger

2. Direct Integration of a Micro Turbine and a SOFC

1.2 Motivation for the present work

Fuel cells have the potential for high efficiency energy conversion, and they are very well suited to operate on hydrogen. Consequently, this technology appears to be very suitable for a post-fossil-fuel based energy economy. However, the transition from a fossil fuel based energy system to a hydrogen based system is complicated and will take time. The SOFC suits well into this perspective, as it is the most applicable fuel cell type for both fossil fuels and hydrogen. Furthermore, the high operating temperature of SOFCs facilitates the combination with gas- and steam turbines to reach electrical efficiencies beyond the limitations of conventional technologies. Fuel cells in general are able to achieve high efficiencies even for small units, and this makes them very suitable for distributed generation. SOFC/GT power plants have been suggested for several applications such as stand-alone power plants, distributed generation, large scale power production and marine propulsion.
An experimental investigation of this system for performance evaluation is very expensive. In this respect, mathematical modeling of system and its simulation on computer proves to be very inexpensive.

1.3 Organization of the report

This report presents the work of my master's thesis based upon gas turbine and solid oxide fuel cell hybrid system, which is a part of the curriculum of master of engineering program. The

report deals with the zero dimensional modeling of gas turbine and solid oxide fuel cell and simulation of the system based upon the developed modeling.

The report has been sub divided into seven chapters, chapter one deals with the introductory part of the gas turbines, fuel cell and hybrid system in brief and explains the reasons of motivation. In chapter two, a detailed review of literatures is presented. These literatures explain about the advancements and developments in the field of fuel cells, gas turbines and, gas turbine and fuel cell hybrid system. The literatures discussed are presented in a manner, which not only provides the notions about the developments in the respective field, but these build the basic knowledge of the system also.

After the discussion of literature review, conclusion drawn from it and objective of the present work is elucidated. In chapter 3, a detailed study about the fuel cell is presented. It explains about the fuel cell, types of fuel cell and solid oxide fuel cell in detail. After a theoretical discussion about the fuel cell, formulation of fuel cell is explained. To evaluate the performance of fuel cell through mathematical modeling, these formulations are used. Analogous to chapter 3, formulation of gas turbine power plant is explained in chapter 4. Each component of gas turbine power plant (such as gas turbine, compressor, and Combustion chamber etc.) is modeled separately using control volume approach with mentioned assumptions. Chapter 5 deals with the introduction of hybrid system. It explains the method and technique to combine a fuel cell with a gas turbine. All the methods of combining a gas turbine with solid oxide fuel cell are discussed with the help of neat sketches. In chapter 6, solution methodology has been discussed for the analysis of model. In chapter 7, results obtained from simulation of gas turbine and solid oxide fuel cell hybrid system, based upon the model developed in EES (Engineering Equation solver) software, are explained. Finally in Chapter 8, conclusion drawn from the thesis work and scope for future work are explained in detail.

Chapter 2

Literature Review

Gas turbine and fuel cell system are an extensive area of research, in which several researchers have already made some mark and several others are indulging themselves in this direction. Literature survey for project is enlisted here. For sake of convenience, literature review has been divided into three groups: Fuel cell power plant system, Gas turbine power plant system and Gas turbine and fuel cell hybrid power system.

2.1 Classification of literature review

(1) Fuel cell power plant system
(2) Gas turbine power plant system
(3) Gas turbine and fuel cell hybrid power system

2.1.1 Fuel cell power plant system

Fuel cell is an electrochemical device which converts fuel (e.g. hydrogen) directly to electricity without undergoing combustion. Fuel cell technology is suitably integrated into the renewable energy scheme [1]. Fuel cells are an ideal means for generating electrical power and can provide benefit to the stationary power sector due to their, high efficiency in both part load and full load performance, ability to produce electrical power without combustion or rotating machinery, capability to function with cogeneration technologies, i.e., power and thermal energy production, and low non-combustion pollution level[2].

The common types of fuel cells are phosphoric acid (PAFC), molten carbonate (MCFC), proton exchange membrane (PEM) and solid oxide (SOFC), all named after their electrolytes. Because of their different materials and operating temperatures, they have varying benefits, applications and challenges, but all share the potential for high electrical efficiency and low emissions. Because they operate at sufficiently low temperatures they produce essentially no NO_x, and because they cannot tolerate sulfur and use desulfurized fuel they produce no SO_x. Because they

rely on electrochemical reactions instead of combustion, fuel cells need an easily oxidized substance, such as hydrogen. Some fuel cells, such as solid oxide fuel cells (SOFC), can also utilize carbon monoxide (CO). This makes them more fuel flexible and also generally more efficient with available fuels, such as natural gas or propane. Hydrogen and CO can be produced from natural gas and other fuels by steam reforming, for example. Fuel cells like SOFCs that can reform natural gas internally have significant advantages in efficiency and simplicity when using natural gas because they do not need an external reformer[3].

Solid oxide fuel cells (SOFCs) have been considered in the last years as one of the most promising technologies for very high-efficiency electric energy generation from natural gas, both with simple fuel cell plants and with integrated gas turbine-fuel cell systems. Among the SOFC technologies, tubular SOFC stacks with internal reforming have emerged as one of the most mature technology, with a serious potential for a future commercialization. A model is calibrated on the available data for a recently demonstrated tubular SOFC prototype plant. The model applies to a tubular SOFC stack fed with natural gas with internal reforming. The model calculates: thermodynamic properties and chemical composition of anode and cathode outlet and stack exhaust gases, SOFC thermal balance (efficiency, heat generated), SOFC second law analysis (entropy losses), as a function of fuel and air utilization, of the inlet compositions and average working temperature. The analysis of model reported an electrical efficiency of 52% based upon LHV of fuel. The discussion of the results of the thermodynamic and parametric analysis yields interesting considerations about partial load SOFC operation and load regulation, and about system design and integration with gas turbine cycles[4].

A semi-empirical model presented that can be used to evaluate the performance of a proton exchange membrane (PEM) fuel cell, with less calculation than other models presented in literature [5].The PEM fuel cell operates at a lower temperature [6] (<100°C) [7].An empirical model of a PEM fuel cell has been developed to simulate the performance of fuel cells without extensive calculations and the effect of operating conditions on the cell performance has been investigated [8].

The solid oxide fuel cell (SOFC) is one of the most promising fuel cells for direct conversion of chemical energy to electrical energy with the possibility of its use in co-generation system because of high temperature waste heat. The SOFC operates at 600-1000℃ where the ceramic electrolyte becomes conductive to oxygen ions, but nonconductive to electrons [9]. For modeling of a fuel cell a detailed review of modeling approach is explained in[9].One of the major advantage offered by the SOFC is, it offers a greater fuel flexibility; means fuel can be a mixture of hydrogen, methane, carbon monoxide and some other higher hydrocarbons. The effects of different variables (such as fuel utilization efficiency, air to fuel ratio etc.) on the plant efficiency of SOFC power plant has studied by [10].

An analytical model of a micro solid oxide fuel cell (SOFC) system fed by butane is introduced and analyzed in order to optimize its exergetic efficiency. The performance of SOFC micro power plant is calculated using operational parameters based on experimental results of several recent studies by [11].

Two different computational models developed for the electrical performance of the tubular SOFC designed by Siemens Westinghouse Corporation. The results of both the methods are in good agreement with the experimentally quoted data. A relatively simple analytical procedure can be used to predict the performance of cell as a function of cell dimensions [12].

The tubular solid oxide fuel cell (TSOFC) developed by Siemens Power Generation Inc. (SPGI), is selected .it is considered to be the most advanced design and is approaching commercialization. A computer simulation model of the SPGI 100 kW AC CHP (combined heat and power) TSOFC stack was developed using Aspen Plus®. The optimum realistic net electrical efficiency of the plant ranging between 36.1 to 37.8 % was identified [13].

2.1.2 Gas turbine power plant system

The Gas turbines have been used to produce power for many years. They are the main source of power for jet aircraft and can be used to create industrial power in gas turbine power plants. The concept is similar to that of a combustion engine: to convert chemical energy of a fuel into mechanical energy. The fluid cycle is similar to a combustion engine. A working fluid (usually

air) is compressed, fuel is added and the mixture is ignited to initiate combustion. The combustion releases energy and the fluid expands moving a physical barrier. The moving of the barrier is the mechanical work out of the cycle. A portion of this mechanical energy is then used to compress the fluid in the next cycle. The difference between a gas turbine and a combustion engine is that the gas turbine cycle runs continuously instead of in iterative cycles (one after the other). The basic components of a gas turbine are a compressor, combustor or heat exchanger, and a turbine [14].

The gas turbine engine is known to have a number of attractive features, principally: low capital cost, compact size, short delivery, high flexibility and reliability, fast starting and loading, lower manpower operating needs and better environmental performance in relation to other prime movers, especially the steam turbine plant, with which it competes. However, it suffers from limited efficiency, especially at part load. Cogeneration, on the other hand, is a simultaneous production of power and thermal energy when the otherwise wasted energy in the exhaust gases is utilized. Hence, cogeneration with gas turbines utilizes the engine's relative merits and boosts its thermal efficiency. Thereby, the worldwide concern about the cost and efficient use of energy is going to provide continuing opportunities, for gas turbine cogeneration systems, in power and industry [15]. A comparison of various possible cogeneration schemes for gas turbine power plant has explained by [15].

Another method of improving the efficiency of a gas turbine power plant system is to reduce the air inlet temperature. Adding an inlet air pre-cooler connected to the evaporator of an aqua ammonia absorption chiller which is driven by the tail-end heat recovered from the engine exhaust gases. A heat recovery boiler is used to partly recover the exhaust heat before entering the generator of the chiller. The performance of this combined system, namely power, efficiency and specific fuel consumption is studied and compared with the simple cycle. The variables in this parametric study are mainly compressor pressure ratio, turbine inlet temperature (TIT) and ambient Temperature. Result shows that the combined system achieves gains in power, overall efficiency, and overall fuel consumption, of about 21.5, 38 and 27.7%. The performance of the combined system shows less sensitivity to variations in operating variables [16].Gas turbines with air–water mixtures as the working fluid promise high electrical efficiencies and high

specific power outputs to specific investment costs below that of combined cycles. Different humidified gas turbine cycles have been proposed, for example direct water-injected cycles, steam-injected cycles and evaporative cycles with humidification towers. However, only a few of these cycles have been implemented and even fewer are available commercially. The basic idea of gas turbine humidification is that the injected water or steam increases the mass flow rate through the turbine. This augments the specific power output, since the compressor work remains constant (i.e. if water is injected after the compressor) and much less work is required to increase the pressure of a liquid than a gas[17].

A straightforward modification of the simple gas turbine cycle is to utilize the waste heat available at turbine exit by means of a heat exchanger or recuperator. A recuperator is a heat exchanger located in a gas turbine exhaust. It enables to transfer the heat from heat available in turbine exhaust gases to the combustor inlet air, consequentially increasing the temperature of the combustion inlet air and reduces the amount of fuel required to reach the desired TIT. It reduces specific fuel consumption compared to a conventional simple cycle gas turbine, while ensuring exhaust temperature is still suitable for CHP. The biggest challenge to the designer of heat exchangers is in the small engine class (micro-turbines); efficiencies over 30% can then be achieved. Gas turbine cycles with heat recovery are generally known as advanced cycles. Heat recovery schemes (recuperators or regenerators) are one of the most important ways increasing the efficiency of the power generation process by more than 40%; they also result in lower levels of pollution for a given output of electricity[18]. Pilavachi [18] has discussed some examples of developments/modifications to the gas turbine such as, increased TIT, waste heat recuperation, steam or water injection, combined cycle etc. to reach to a conclusion of higher efficiency obtainable from gas turbine system.

2.1.3 Gas turbine and fuel cell hybrid power system

The current concern with the consumption of fossil fuels and pollutant emissions (especially green house gases such as CO_2) is the main motivator for the exploration of fuel cell systems as an alternative to traditional power generation systems. Solid oxide fuel cell (SOFC) hybridization with micro gas turbine (MGT) is an attractive option for power generation up to a

few MW. Electrochemical means of energy conversion (such as fuel cells) make it possible to achieve higher efficiencies than in conventional thermal cycles, because they are not limited by theoretical Carnot efficiency [19].

In a close future, aircraft will probably consume a greater amount of electric power than present ones and will be subject to more severe environmental laws. These factors will demand a reformulation of the power production model, aiming at a system of increased power, more cost effective and with lower emissions. Solid oxide fuel cell (SOFC) micro turbine hybrid systems are a promising option for this reformulation, but it will be necessary to adequate them to the aerospace requirements[7]. Solid oxide fuel cell (SOFC) stacks are at the core of complex and efficient energy conversion systems for distributed power generation. Such systems are currently in various stages of development. These power plants of the future feature complicated configurations, because the fuel cell demands for a complex balance of plant. Moreover, proposed SOFC-based systems for stationary applications are often connected to additional components and subsystems, such as a gasifier with its gas-cleaning section, a gas turbine, and a heat recovery system for thermal cogeneration or additional power production[20].

Power generation using gas turbine (GT) power plants operating on the Brayton cycle suffers from low efficiencies, resulting in poor fuel to power conversion. A solid oxide fuel cell (SOFC) is proposed for integration into a 10MWgas turbine power plant, operating at 30% efficiency, in order to improve system efficiencies and economics. The SOFC system is indirectly coupled to the gas turbine power plant, paying careful attention to minimize the disruption to the GT operation. A thermo-economic model is developed for the hybrid power plant, and predicted an optimized power output of 20.6MWat 49.9% efficiency [21]. The advantages of these modern power plants are high electrical efficiency and low emissions. SOFC cogeneration systems achieved 46% electrical efficiency working at 1 atm. Pressure and SOFC/GT hybrid systems achieved 53% electrical efficiency working at 3 atm. Pressure. The next target for SOFC/GT hybrid system is to achieve 55-60% electrical efficiency [22]

A conceptually designed 30 kW capacity SOFC hybrid micro generation system has been investigated for its use in small distributed energy systems. Firstly the design-point and part-load

characteristics were investigated, and then part load performance of the system has been evaluated under two different operating modes of gas turbine. In these typical operating modes, i.e. constant and variable rotation speed gas turbine operation has considered and found that variable sped mode is more advantageous to performance degradation under part load condition[23].

For a 200 kW power plant in which the fuel cell accounts for approximately three quarters of the generated power (149 kW) and the gas turbine one quarter (50 kW). The total system efficiency based upon electrical output of the design was calculated to be 43.4% [24]. A comparison with the efficiency of simple gas turbine cycle and regenerative gas turbine cycle shows the superiority of SOFC power plant for the considered electrical power range [25]. Methane fed hybrid SOFC-GT power generation system of capacity 1.25 MW is successfully modeled. It has been demonstrated that SOFC-GT can achieve 60% net electrical efficiencies and it is feasible for SOFC to be integrated with a gas turbine engine. If we consider the recuperation at the downstream of the gas turbine, efficiencies can be further improved [26].

A Hybrid System based on High Temperature Fuel Cells coupled to a Micro turbine allows a high efficiency, low environmental pollution and it may be exploited as a CHP System producing heat and electricity both Grid Connected and Stand Alone; the overall electrical efficiency could reach a very high value (up to 60%) and total efficiency could be over 70% including the contribution due to heat recovery. The steady state simulation of the Hybrid System shown that the efficiency both of the Electrochemical Unit and of the whole Hybrid System can be higher than that of gas-steam turbine conventional power plant [27]. The overall thermal efficiency and specific power output of the hybrid gas turbine system was determined from a control-volume analysis using the first and second laws of thermodynamics. The cycle achieved a thermal efficiency of 64.1% at a pressure ratio of 14. The specific power output was found to be 520 W/kg s [28].

For a solid oxide fuel cell (SOFC) integrated into a micro gas turbine (MGT) hybrid power system, SOFC operating temperature and turbine inlet temperature are the key parameters, which affect the performance of the hybrid system. Thus, a least squares support vector machine (LS-

SVM) identification model based on an improved particle swarm optimization (PSO) algorithm is proposed to describe the nonlinear temperature dynamic properties of the SOFC/MGT hybrid system by the author in his research paper. During the process of modeling, an improved PSO algorithm is employed to optimize the parameters of the LS-SVM. In order to obtain the training and prediction data to identify the modified LS-SVM model, a SOFC/MGT physical model is established via Simulink toolbox of MATLAB6.5. Compared to the conventional BP neural network and the standard LS-SVM, the simulation results show that the modified LS-SVM model can efficiently reflect the temperature response of the SOFC/MGT hybrid system[29].

A novel concept for integrating fuel cells with desalination systems is proposed and investigated. Two unique case studies were discussed; the first involving a hybrid system with a reverse osmosis (RO) unit and the second: integrating with a thermal desalination process such as multi-stage flash (MSF). The exhaust gas from a hybrid power plant (fuel cell/turbine system) utilized for desalination units. This system global efficiency was found to be 76.69% that meets the US DOE's (United States Department of Energy) goal of lower heating value efficiency above 70% [30].

A system level modelling study of three combined heat and power systems based on biomass gasification is available. Product gas is converted in a micro gas turbine (MGT) in the first system, in a solid oxide fuel cell (SOFC) in the second system and in a combined SOFC–MGT arrangement in the third system. An electrochemical model of the SOFC has been developed and calibrated against published data from Topsoe Fuel Cells A/S and the Riso National Laboratory. The SOFC converts the syngas more efficiently than the MGT, which is reflected by the energetic electrical efficiency of the gasifier and MGT system in opposition to the gasifier and SOFC configuration. By combining the SOFC and MGT, the unconverted syngas from the SOFC is utilized in the MGT to produce more power and the SOFC is pressurized, which improves the efficiency to as much as η_{el} = 50.3% [31].

A gas turbine and fuel cell hybrid plant scheduled to go online in the year 2012, and will achieve an efficiency of around 70% [32]. A critical survey of thermal efficiencies of combined SOFC-GT in past literatures adopted from [33] is listed in Table 2.1.

Table 2.1: Survey of Thermal Efficiencies

System configuration	Efficiency	Reference
Pressurized cycle using an SOFC and integrated GT bottoming cycle	68.10	Harvey and Richter [34, 35]
Gasification process linked with an SOFC and GT	60.00	Lobachyov and Richter [36]
Pressurized SOFC–GT combined cycle	60–65	George [37]
Pressurized SOFC–GT cycle with a heat recovery bottoming cycle	70<	Campanari and Macchi [38]
500 kW with GT reheat and air compression inter-cooling	65<	Palsson et al. [39]
Recuperated micro gas turbine (MGT) with a high temperature SOFC	60<	Costamagna et al. [40]
SOFC stack, combustor, GT, two compressors and 3 recuperators	60<	Chan et al. [41]
50 kW microturbine coupled with a high-temperature SOFC	60.00	Massardo et al. [42]
Pressurized tubular SOFC combined with an intercooled-rehear GT	66.23	Rao and Samuelsen [43]
Humid air turbine (HAT) cycle incorporated with the above cycle	69.05	Rao and Samuelsen [43]
Dual SOFC–HAT hybrid cycle	75.98	Rao and Samuelsen [43]
Internal-reforming (IR) SOFC–GT power generation system	60<	Chan et al. [44]
Combined SOFC–GT system with liquefaction recovery of CO2	70.64	Inui et al. [45]
30 kW MGT–SOFC hybrid system	65.00	Uechi et al. [46]
IR tubular SOFC–GT plant with 3 heat exchangers and mixers	65.4	Calise et al. [47]
1.5 MW integrated IRSOFC with two GTs and one HRSG	60.00	Calise et al. [48]
Two-staged low and high temperature SOFC power generation cycle	56.10	Araki et al. [49]
Multi-staged SOFC–gas turbine–CO2 recovery power plant	68.50	Araki et al. [50]
Recuperated GT integrated with SOFC	59.4	Tse et al. [51]
Recuperated GT with compressor air inter-cooling and two SOFCs	68.7	Tse et al. [51]
Recuperated GT integrated with SOFC	60.6	Haseli et al. [33]

2.2 Conclusions from literature review

Solid oxide fuel cells (SOFC) are considered prime candidates for stationary power generation in the intermediate to long-term future. In addition to its clean and efficient operation, its high temperature of operation (800–1100 K) allows for use of a wide range of fuels (including CO), up to few MW power generation and for CHP application SOFC's are the best option to combine with gas turbine system. The combine system offers a very high electrical efficiency ranging between 60 – 70% and with the advancement in the technology very soon these systems will achieve the targeted efficiency (75%).

Recent interest in the field of gas turbine and solid oxide fuel cell hybrid system applications for the power industry has led to the need for accurate computer simulation models to aid in system design and performance evaluation.

2.3 Objective of present work

The purpose of the present work is to promote the near term realization of high efficiency decentralized power plants. The present research work has been performed to achieve the following objectives:

1. To find best configuration of integrated gas turbine and solid oxide fuel cell hybrid system power plant from the available configurations.
2. Thermodynamic modeling, simulation and performance evaluation of integrated gas turbine and solid oxide fuel cell hybrid system power plant using natural gas.
3. Parametric study of this system using first and second law of thermodynamics.

In past sections we discussed about the fuel cell, gas turbine and combined gas turbine and fuel cell system. In this chapter we will discuss about fuel cell in detail and develop a formulation for modeling and simulation of fuel cell. We will first discuss fuel cell, types of cell and then about the formulation of the fuel cell.

3.1 Fuel cell

Fuel cells are electrochemical devices that convert the chemical energy of the fuel directly into electrical energy. The generic fuel cell basically consists of an electrolyte layer sandwiched between a porous anode and cathode electrode.

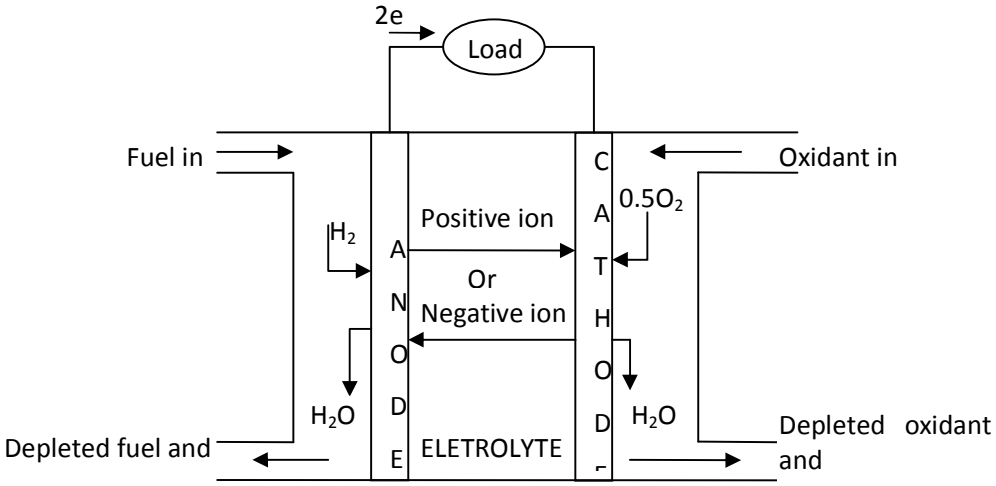

Figure3.1: Description of Fuel Cell

A schematic representation of a fuel cell with all these parts is shown in Figure3.1. In a typical fuel cell, fuel[1] is fed continuously to the anode compartment (negative electrode) and an oxidant[2]

[1] The fuel is reformed before feeding into anode compartment if, fuel is not pure hydrogen.

is fed continuously to the cathode (positive electrode) compartment; the electrochemical reaction takes place at the electrodes to produce the current[3]. The hydrogen fuel and oxygen combines to produce electricity, heat and water. Heat is released due to exothermic electrochemical reaction. A catalyst [4] presents between in electrode and electrolyte splits the hydrogen into two parts a proton and an electron. The protons travel through the electrolyte to the cathode. The electron cannot pass through the electrolyte so they must flow through an external circuit, creating a DC circuit. The electron finally arrives at cathode where they recombine with the hydrogen and oxidant (i.e. oxygen). Heat and water is thus produced.

3.2 Types of Fuel cell

Fuel cells are classified primarily on the basis of electrolyte they employ. This determines the kind of chemical reactions that take place in the cell, the kind of catalysts required, the temperature range in which the cell operates, the fuel required, and other factors. These characteristics, in turn, affect the applications for which these cells are most suitable.

There are 5 major types of fuel cells currently under development:

1. Alkaline fuel cell (AFC)
2. Polymer electrolyte membrane fuel cell (PEMFC)
3. Phosphoric acid fuel cell (PAFC)
4. Molten carbonate fuel cell (MCFC)
5. Solid oxide fuel cell (SOFC)

Each type of cell has its own characteristics, limitations, advantageous, and application which has been tabulated in table 3.1.

---

[2] The oxidant is oxygen which is taken from air; pure oxygen can be also supplied.

[3] Current is strictly defined as motion of a charged specie and can be in the form of anions (negatively charged species such as O^{2-}), cations (positively charged species such as H^{+}), or negatively charged electrons.

[4] The material of catalyst depends upon the electrolyte used; it could be made of platinum, nickel, perovskites.

Table 3.1: Type of fuel cell and properties [52-53]

Fuel cell Type	Operating Temperature	Efficiency	Charge carrier	Electrolyte	Catalyst	Product water management
Alkaline Fuel cell (AFC)	60-70℃	36%	OH^-	Aqueous solution of potassium hydroxide soaked in a matrix	Platinum	Evaporative
Proton Exchange Membrane Fuel cell (PEMFC)	85-105℃	40%	H^+	Solid organic polymer poly-perfluorosulphuric acid	Platinum	Evaporative
Phosphoric Acid Fuel cell (PAFC)	160-220℃	40-45%	H^+	Liquid phosphoric acid soaked in a matrix	Platinum	Evaporative
Molten carbon Fuel cell (MCFC)	600-650℃	45-47%	$CO3^=$	Liquid solution of lithium, sodium and/or potassium carbonate soaked in a matrix	Nickel	Gaseous product
Solid oxide fuel cell (SOFC)	800-1000℃	48-55%	$O^=$	zirconium Solid oxide to which a Small amount of ytrria is added	Perovskites	Gaseous product

Form table 3.1 we can conclude that the MCFC and SOFC are the fuel cell that has a high operating temperatures i.e.600-660^{o}C for MCFC and 900-1100^{o}C for SOFC. Due to these reasons these fuel cells are preferred for the gas turbine and fuel cell hybrid system. The SOFC has a quite high operating temperature than all the other fuel cells and it also offers a very high efficiency than other fuel cells. Because of the high operating temperature and high efficiency characteristic of the SOFC, this fuel cell is generally preferred for the hybrid system technology.

3.2.1 Solid oxide fuel cell (SOFC)

Solid oxide fuel cell (SOFC) systems have been recognized as the most advanced power generation system with the highest thermal efficiency with a compatibility with wide variety of hydrocarbon fuels, synthetic gas from coal, hydrogen, etc. [54]. A SOFC is a continuously fed electrochemical cell, where the electrodes and electrolyte are ceramic materials. The major

electrochemical reaction which takes place in an SOFC is the oxidation of fuel. A large variety of materials are used in SOFCs and novelSolid oxide fuel cells employ a solid oxide material as an electrolyte [55]. The material used for electrolyte is Yttria(Y_2O_2) stabilized Zirconia(ZrO_2) and perovskites is used as catalyst. The SOFC is a straightforward two-phase gas-solid system so it has no problems with water management, flooding of the catalyst layer, or slow oxygen reduction kinetics. Internal reforming in SOFCs is possible over the anode catalyst, also partial oxidation reactions and direct oxidation of the fuel have been found to occur. Different concepts for solid oxide fuel cells have been developed over the years. Flat plates have an easier stack possibility while tubular designs have a smaller sealing problem. Monolithic plate and even single-chamber designs have been considered and investigated for SOFC use. Due to the high power density of SOFCs compact designs are feasible. An important advantage of SOFCs is the internal reforming.

3.2.2 SOFC Design

There are three types of SOFC designs are available:

1. Tubular type

2. Planar type

3. The HEXIS (Heat Exchange Integrated System) tubular concept for SOFC (under development)

3.3 Fuel cell stacking

A single fuel cell theoretically can be made to achieve desired current and power output simply by increasing the active surface area of the electrode and flow rate of reactants. However, the output voltage of a single fuel cell is limited by the fundamental electrochemical potential of the reacting species involved and it is always less than 1V for real operating condition. Therefore to achieve a higher voltage and a compact design, a fuel cell stack of several individual cells connected in series are utilized. For a stack in series, the total current is proportional to the active

electrode area of each cell in stack and is the same through all cells in series. The total stack voltage is simply the sum of individual cells. For fuel cell in parallel, the current is additive and the voltage is the same in each cell. The combination of parallel and series is also used. The no. of stack is determined by the following equation:

$$N_s = \frac{N_{cell}}{N_{cell}^{stack}} \tag{3.1}$$

$$N_{cell} = \frac{A_T}{A_c} \tag{3.2}$$

$$A_T = \frac{I}{i} \tag{3.3}$$

$$V_s = N_{cell}^{stack} \times V_{cell} \tag{3.4}$$

3.4 Electrochemical reaction

When an electrochemical reaction takes place, the overall global ruction and thus the chemical energy difference between the beginning and the end states of the reactant and products are identical to the analogous chemical reaction. However, an electrochemical reaction circulates current through a continuous circuit to complete the reaction, while a purely chemical reaction does not. The electrochemical reaction for hydrogen and methane are as follows:

For hydrogen

Anode:

$$H_2 \rightarrow 2H^+ + 2e^- \tag{3.5}$$

Cathode:

$$2H^+ + 2e^- + \frac{1}{2}O_2 \rightarrow H_2O \tag{3.6}$$

Overall:

$$H_2 + \frac{1}{2}O_2 \rightarrow H_2O \tag{3.7}$$

For methane

Reforming Reaction:

$$CH_4 + 2H_2O \rightarrow 4H_2 + CO_2 \tag{3.8}$$

Anode:

$$CH_4 + 4O \rightarrow 2H_2O + CO_2 + 8e \tag{3.9}$$

Cathode:

$$\frac{1}{2}O_2 + 2e \rightarrow O \tag{3.10}$$

Overall:

$$CH_4 + 2O_2 \rightarrow 2H_2O + CO_2 \tag{3.11}$$

3.4.1 Consumption and production of species

This section answer to an important question: how much mass of a given reactant is required to produce the required amount of current? Conversely, how much current is required to produce a certain amount of product? The production and consumption of species are governed by the Faraday's law of electrolysis:

1. For a specific charged passed, the mass of the products formed are proportional to the electrochemical equivalent weight of the products.

2. The amount of product formed or reactant consumed is directly proportional to the charge passed.

The second law is the most important for fuel cell study. The current generated is proportional to the mass reacted or produced:

$$m \propto I \tag{3.12}$$

Considering a purely electrochemical reaction, rate of molar Consumption or production of species x (mol of x/s) given as:

$$\dot{n}_x = \frac{iA_T}{nF} = \frac{I}{nF} \tag{3.13}$$

3.4.2 Measure of reactant utilization efficiency

Faradic efficiency: it is the measure of the percent utilization of reactant in galvanic process:

$$\varepsilon_f = \frac{theoretical\ required\ rate\ of\ reactant\ supplied}{actual\ rate\ of\ reactant\ supplied} \tag{3.14}$$

When applied to the fuel in a galvanic redox reaction the Faradic efficiency is known as fuel utilization efficiency:

$$\mu_f = \frac{theoretical\ required\ rate\ of\ fuel\ supplied}{actual\ rate\ of\ fuel\ supplied} \tag{3.15}$$

In case of electrolytic process, some side reaction takes place and inefficiencies may occur, which results in less than a complete conversion. The current efficiency is defined as:

$$\varepsilon_f = \frac{actual\ rate\ of\ species\ reacted\ or\ produced}{theoretical\ rate\ of\ species\ reacted\ or\ produced} \tag{3.16}$$

3.4.4 Stoichiometric ratio

Cathodic Stoichiometric ratio is defined as:

$$\lambda_c = \frac{1}{\varepsilon_{f,c}} = \frac{actual\ rate\ of\ oxidizer\ delivered\ to\ cathode}{theoretical\ rate\ of\ oxidizer\ required} \tag{3.17}$$

Anodic Stoichiometric ratio is defined as:

$$\lambda_a = \frac{1}{\varepsilon_{f,a}} = \frac{actual\ rate\ of\ fuel\ delivered\ to\ anode}{theoretical\ rate\ of\ fuel\ required} \tag{3.18}$$

3.4.5 Flow stoichiometry

Due to inefficiency in reactant utilization, the molar flow rate of reactant is given as:

$$\dot{n}_{in} = \lambda_i \frac{iA_T}{nF} = \lambda_i \frac{I}{nF} \tag{3.19}$$

The consumption of reactant is evaluated by using Faraday's law as stated above is rewritten here

$$\dot{n}_{consumed} = \frac{iA_T}{nF} = \frac{I}{nF} \tag{3.20}$$

Therefore the amount of reactant out of a fuel cell is

$$\dot{n}_{out} = \dot{n}_{in} - \dot{n}_{consumed} = (\lambda_i - 1)\frac{iA_T}{nF} \tag{3.21}$$

3.5 Calculation of voltage

3.5.1 Calculation of maximum expected voltage (Eo):

Invoking first law of thermodynamics for a simple compressible system

$$dU = \delta Q - \delta W \tag{3.22}$$

The work can be divided into mechanical expansion work and electrical work:

$$\delta W = \delta W_p + \delta W_e = PdV + \delta W_e \tag{3.23}$$

For a reversible system, second law of thermodynamics can be given as

$$\delta Q = TdS \tag{3.24}$$

The differential change in the Gibbs free energy is given as:

$$dG = dH - TdS - SdT \tag{3.25}$$

For a constant temperature process equation (3.24) becomes

$$dG = dH - TdS \tag{3.26}$$

The differential change in enthalpy for a given reaction is

$$dH = dU + PdV + VdP \tag{3.27}$$

For a constant presure process, the differential change in enthalpy is

$$dH = dU + PdV \tag{3.28}$$

Now, subsitttuting eq. (3.23) and (3.22) in (3.21) we get,

$$dU = TdS - \delta W_e - PdV \tag{3.29}$$

Now by subsittution of eq. (3.27) and (3.28) into (3.25), we can show that

$$-dG = \delta W_e \tag{3.30}$$

Since the equation (3.29) has been derived for a reversible system, it is an expression of the maxium electrical work possible from the system. Now consider the work required to move a given charge:

$$w_e = nFE^o \tag{3.31}$$

It should to be noted here, that E^o is not energy; it is voltage. Combining equations (3.31) and (3.30) E^o can be written as:

$$E^o = -\frac{\Delta G}{nF} \tag{3.32}$$

This is the maximum possible reversible voltage of an electrochemical cell and E^o is also called the reversible voltage.

3.5.2 Calculation of thermal voltage (E^{oo}):

When all the potential chemical energy for a reaction went into electrical work, if there were no heat transfer, there were no entropy changes (i.e. reversible adiabatic process); form equation (3.25) $dG = dH$. In this case:

$$E^{oo} = -\frac{\Delta H}{nF} \tag{3.33}$$

This is the maximum voltage for a reversible adiabatic system. It is also known as the thermal voltage.

3.5.3 Calculation of thermodynamic cell efficiency (ηth):

The thermodynamic efficiency of a fuel cell is defined as the ratio of actual electrical work to maximum

$$\eta_{th,max} = \frac{E^o}{E^{oo}} = \frac{-\Delta G/nF}{-\Delta H/nF} = \frac{\Delta H - T\Delta S}{\Delta H} \tag{3.34}$$

The equation (3.34) can be rearranged as:

$$\eta_{th,max} = 1 - \frac{T\Delta S}{\Delta H} \tag{3.35}$$

3.5.4 Calculation of Nernst voltage (E):

Since the enthalpy is a function of only temperature it can be easily concluded that the thermal voltage (E^{oo}) is also a function of temperature alone, while the reversible voltage (E^o) is actually a function of temperature and pressure of the reactant and products. The Nernst equation

is an expression of the maximum possible open circuit voltage[5] as function of temperature and pressure and is an expression of an established thermodynamic equilibrium. Consider a global redox reaction in a fuel cell:

$$v_A A + v_B \leftrightarrow v_C C + v_D D \tag{3.36}$$

Where the $v's$ are the stoichiometric coefficients of the balanced electrochemical reaction. From thermodynamics of systems in equilibrium:

$$\Delta G = \Delta G(T) - R_u T \, ln\left[\frac{a_A^{vA} \; a_B^{vB}}{a_C^{vC} a_D^{vD}}\right] \tag{3.37}$$

Where the a's are the thermodynamic activity coefficients for the reacting specie. To convert above equation in voltage form, dividing by nF:

$$E(T,P) = E = -\frac{\Delta G}{nF} + \frac{R_u T}{nF} ln\left[\frac{a_A^{vA} \; a_B^{vB}}{a_C^{vC} a_D^{vD}}\right] \tag{3.38}$$

This equation is known as General Nernst voltage expression. By using this we can write Nernst voltage equation for variety of fuels. The expression for hydrogen and methane are given below: Nernst voltage expression for hydrogen fuel cell

$$E = E^0 + \frac{R_u T}{2F} ln\left[\frac{P_{H_2} P_{O_2}^{1/2}}{P_{H_2O}}\right] \tag{3.39}$$

Nernst voltage expression for methane fuel cell

$$E = E^0 + \frac{R_u T}{8F} ln\left[\frac{P_{CH_4} P_{O_2}^2}{P_{H_2O}^2 P_{CO_2}}\right] \tag{3.40}$$

[5] The voltage available at the zero cells current is termed as the open circuit voltage.

3.6 Polarization curve:

It represents the cell voltage-current relationship for evaluation of fuel cell performance. Polarization curve is a very important tool for studying the complete performance of any fuel cell. The polarization curve is generally plotted between cell voltage and current density instead of voltage and total current. A polarization curve plotted between cell voltage and current density of the fuel cell is shown in Fig3.1. The graph show in the Fig3.1 has been plotted for a polymer electrolyte membrane fuel cell in EES. There are five types of losses which results in departure from maximum thermal voltage to actual cell voltage:

3. Losses due to entropy change which cannot be engineered.

2. Losses due to activation overpotential at the electrodes.

3. Losses due to Ohmic polarization. These are the resistive losses which include all electrical and ionic conduction losses through the electrolyte, catalyst layer, cell interconnects, and contacts.

4. Losses due to concentration polarization of the fuel cell, caused by the mass transport limitation of the reactant to the electrodes.

5. Losses due to undesired species crossover through electrolyte, internal currents due to leakage of electron through the electrolyte, or any other impurity.

Hence, actual cell voltage is the difference of Nernst voltage and losses, given as:

$$V_{cell} = E - \eta_{a,a} - |\eta_{a,c}| - \eta_{c,a} - |\eta_{c,c}| - \eta_R \tag{3.41}$$

Where, V_{cell} is actual cell voltage, E is theoretical cell voltage, $\eta_{a,a}$ is activation loss at anode, $\eta_{a,c}$ is activation loss at cathode, $\eta_{a,c}$ is concentration loss at anode, $\eta_{c,c}$ is concentration loss at cathode, and η_R is losses due to resistance. These losses have been discussed in detail in next sections.

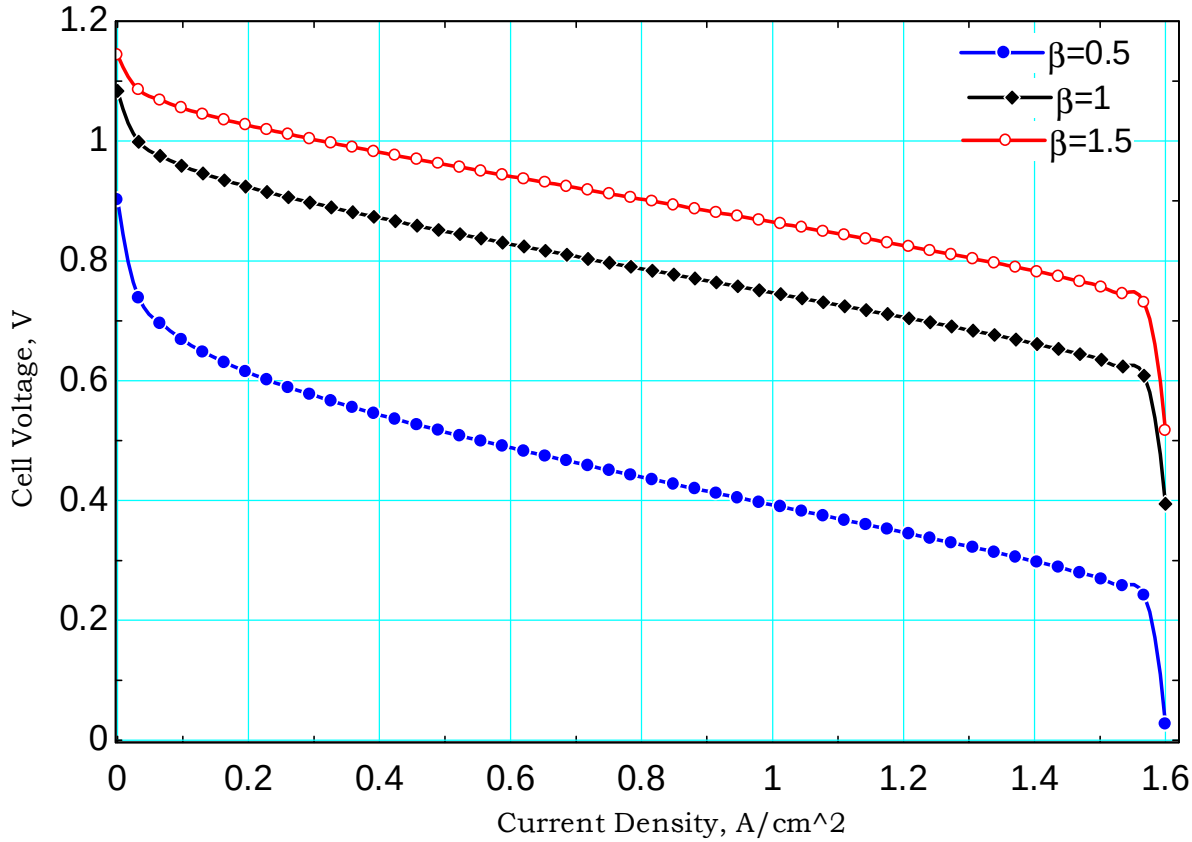

Figure 3.2: Polarization Curve for a Typical Fuel Cell.

3.6.1 Activation polarization (η_a)

Some voltage difference from equilibrium is needed to get the electrochemical reaction going. The activation losses are due to sluggish kinetics of electrochemical reaction. It dominates losses at low current densities. Activation losses are less dominant in case of SOFC due high operating temperature. Physically, the activation losses are the losses required to initiate the reaction. In similar fashion, consider a gasoline vapor and air mixture in combustion chamber, it needs an

ignition energy input for combustion. It is evaluated by using Butler–volmer model of kinetics. Some semi empirical relations are also available. The BV[6] equation is given as:

$$i = i_o \left(\frac{C_s}{C^*}\right)^{\gamma} \left[\exp\left(\frac{\alpha_a F}{R_u T}\eta\right) - \exp\left(\frac{\alpha_c F}{R_u T}\eta\right)\right] \tag{3.42}$$

i is the total fuel cell current density.

i_o is the exchange current density of the electrode of interest and function of reaction concentration.

C_s is the electrode reactant concentration at the catalyst surface.

C^* is the reference concentration of the reactant at STP condition.

γ is the reaction order for elementary charge transfer step, which can vary for different electrodes and reactant and is typically determined experimentally.

$\exp\left(\frac{\alpha_a F}{R_u T}\eta\right)$ is the oxidation reaction at the particular electrode.

$\exp\left(\frac{\alpha_c F}{R_u T}\eta\right)$ is the reduction reaction at the particular electrode.

α_a is the anodic charge transfer coefficient.

α_c is the cathodic charge coefficient.

η is the activation overpotential.

A detailed derivation of the BV equation is available in[56].

[6] BV is an acronym for Buttler-volmer equation

In 1905, based on experimental investigation, Tafel [57] proposed the following relationship between electrode overpotential and current density:

$$\eta = a + blog(i) \tag{3.43}$$

$$a = 2.303\frac{R_u T}{\alpha_j F} log(i_{o)} \tag{3.44}$$

$$b = -2.303\frac{R_u T}{\alpha_j F} \tag{3.45}$$

Where, b is the Tafel slope. Experimentally, the exchange current density and charge transfer coefficient are found with a Tafel plot, which is a plot of log of current exchange density versus overpotential for a given reaction.

3.6.2 Ohmic polarization (η_R)

At moderate current densities, a primarily linear region is evident on the polarization curve. In this region the voltage is affected by the internal resistive losses η_R through the fuel cell, resulting in the nearly a linear behavior, although the activation and polarization losses remains present in this region. The Ohmic polarization is evaluated by using ohm's law:

$$\eta_R = iA\left(\sum_{k=1}^{n} r_k\right) \tag{3.46}$$

For a fuel cell the equation can be written as:

$$\eta_R = i.R_{ohmic} = i\left(R_{anode} + R_{Cathode} + R_{Electrolyte} + R_{Interconnection}\right) \tag{3.47}$$

And R is calculated by using

$$R = \frac{\rho l}{A} \tag{3.48}$$

Where,

R = Resistance (Ω)

ρ = Resistivity (Ωm)

l = Linear path length of ion travel (m)

A = Cross – sectional area of ion travel (m^2)

The resistivity (ρ) is a function of temperature and calculated by using the following relation:

$$\rho = a * exp\left(\frac{b}{T}\right) \tag{3.49}$$

Where, the T is fuel cell operating temperature, a and b are constants. The value of constants depends upon the material of the component. The constants a and b for the tubular SOFC electrode materials (the lanthanum manganite cathode tube, yttria-stabilized zirconia (YSZ) electrolyte, Ni/YSZ anode and doped lanthanum chromite interconnection) [58] are listed in table A. 1 of appendix - A.

3.6.3 Concentration polarization (η_c)

It is caused by the reduction in the reactant surface concentration which dominates the thermodynamic voltage from the Nernst equation and exchange current density from BV equation. The voltage losses due to concentration polarization are determined by using following equation:

$$\eta_c = -\frac{R_u T}{nF} ln\left[1 - \frac{i}{i_L}\right] \tag{3.50}$$

And total concentration polarization is given as:

$$\eta_{c,a} + \eta_{c,c} = -\frac{R_u T}{nF} ln\left[1 - \frac{i}{i_{L,a}}\right] - \frac{R_u T}{nF} ln\left[1 - \frac{i}{i_{L,c}}\right] \tag{3.51}$$

Another semi-empirical approach is often used by replacing the term $\frac{R_u T}{nF}$ with a constant B to better fit with experimental data. Hence equation becomes:

$$\eta_c = -Bln\left[1 - \frac{i}{i_L}\right] \tag{3.52}$$

Therefore total concentration polarization is given as:

$$\eta_{c,a} + \eta_{c,c} = -B_a ln\left[1 - \frac{i}{i_{L,a}}\right] - B_c ln\left[1 - \frac{i}{i_{L,c}}\right] \tag{3.53}$$

Alternate empirical approach a completely empirical approach is also available to calculate the fuel cell concentration polarization:

$$\eta_c = m\exp(ni) \tag{3.54}$$

If this equation is used, the constant m and n are typically fit from several polarization curves, and this single expression includes both anode and cathode concentration polarization.

Limiting current density(i_L): The current density at which cell voltage becomes zero is known as limiting current density. Now, we derive an analytical expression for this value. Assuming one dimensional transport to the catalyst surface:

$$\underbrace{\frac{i_L A}{nF}}_{Consumption} = \underbrace{-D_j A \frac{dC_j}{dx}}_{\substack{Diffusion \\ transport}} + \underbrace{C_j A v_x}_{\substack{Advective \\ transport}} \tag{3.55}$$

If we assume one dimensional flux to the electrode surface in *x* direction with zero bulk flow velocity, we can write:

$$i_L = -nFD_{eff}\frac{C_\infty - C_s}{\delta} \tag{3.56}$$

But the surface concentration C_s is reduced to zero at limiting condition. Hence equation ()

$$i_L = -nFD_{eff}\frac{C_\infty}{\delta} \tag{3.57}$$

Where,

C_∞ known as the concentration of the reactant at the boundary with the flow channel and is calculated by using ideal gas law. It is given as

$$C_\infty = \frac{y_i P}{R_u T} \tag{3.58}$$

D_{eff} = Effective diffusion coefficient

δ = Diffusion layer thickness

3.7 Diffusion coefficient

Knudsen diffusion coefficients for the anode and cathode gases:

$$D_{K,i} = 97 \times r \times \left[\frac{T_{cell}}{M_i}\right]^{0.5} \tag{3.59}$$

Effective Knudsen diffusion coefficients for the anode and cathode gases:

$$D_{K,i(eff)} = D_{K,i} \times \frac{\varepsilon}{\xi} \tag{3.60}$$

Where subscript i represents the gaseous component (H_2, H_2O, O_2 or N_2), r is the electrode pore radius (m), T_{cell} is the cell operating temperature (K), M_i is the molecular weight (kg/kmol) of the gaseous component, ε is porosity and ξ is tortuosity of the electrodes. The ordinary binary diffusion coefficient for both anode and cathode is given as:

$$D_{ik} = \frac{1 \times 10^{-7} \times T_{cell}{}^{1.75} \left(\frac{1}{M_i} + \frac{1}{M_k}\right)^{\frac{1}{2}}}{P\left(v_i^{\frac{1}{3}} + v_k^{\frac{1}{3}}\right)^2} \tag{3.61}$$

Where subscripts i and k represent the gaseous components that make up the binary gas mixture (H_2-H_2O at the anode and O_2-N_2 at the cathode), P is pressure in atmospheres and v is the Fuller diffusion volume listed in table A2 of Appendix – A. the effective ordinary diffusion coefficient is calculated in similar fashion as in case of Knudsen diffusion, which is given as:

$$D_{ik(eff)} = D_{ik} \times \frac{\varepsilon}{\xi} \tag{3.62}$$

The overall effective diffusion coefficient for each gas is given as:

$$\frac{1}{D_{i(eff)}} = \frac{1}{D_{ik(eff)}} + \frac{1}{D_{K,i(eff)}} \tag{3.63}$$

The effective anode and cathode coefficient is given as:

$$D_{An(eff)} = \left(\frac{y_{H_2O}^0 . P}{P}\right) D_{H_2(eff)} + \left(\frac{y_{H_2}^0 . P}{P}\right) D_{H_2O(eff)} \tag{3.64}$$

$$D_{Cat(eff)} = D_{O_2(eff)} \tag{3.65}$$

3.8 Power Output

Power output of the cell is given by the fundamental equation:

$$P = V \times I \tag{3.66}$$

Where,

P is total cell power output,

V is actual cell voltage and

I is total cell current.

3.9 Exergy analysis of fuel cell

Physical exergy at anode and cathode is given as:

Physical exergy at anode inlet:

$$E_{ano,in}^{PH} = h_{i,ano,in} - h_{i,ano,in}^{o} - T_0\left(s_{i,ano,in} - s_{i,ano,in}^{o}\right) \tag{3.67}$$

Physical exergy at cathode inlet:

$$E_{cat,in}^{PH} = h_{i,cat,in} - h_{i,cat,in}^{o} - T_0\left(s_{i,cato,in} - s_{i,cat,in}^{o}\right) \tag{3.68}$$

Physical exergy at anode outlet:

$$E_{ano,out}^{PH} = h_{i,ano,out} - h_{i,ano,out}^{o} - T_0\left(s_{i,ano,out} - s_{i,ano,out}^{o}\right) \tag{3.69}$$

Physical exergy at cathode outlet:

$$E_{cat,out}^{PH} = h_{i,cat,out} - h_{i,cat,out}^{o} - T_0\left(s_{i,cato,out} - s_{i,cat,out}^{o}\right) \tag{3.70}$$

Exergy balance for fuel cell is given as:

$$E_{ano,in}^{PH} + E_{cat,in}^{PH} + E_{cat,in}^{CH} + E_{ano,in}^{CH} = E_{ano,out}^{PH} + E_{ano,out}^{CH} + E_{cat,out}^{PH} + E_{cat,out}^{CH} + \dot{E}_{xd}$$

$$+V_{cell} \times I \tag{3.71}$$

Where, $E_{ano,in}^{PH}$ and $E_{cat,in}^{PH}$ are physical exergy at anode and cathode inlet respectively, $h_{i,ano,in}$ and $h_{i,cat,in}$ are enthalpy of substance at anode and cathode inlet respectively, $h_{i,ano,in}^{o}$ and $h_{i,cat,in}^{o}$ are enthalpy of substance at reference condition corresponding to anode and cathode inlet respectively, $s_{i,ano,in}$ and $s_{i,cato,in}$ are entropy of substance at anode and cathode inlet

respectively, $s^{o}_{i,ano,in}$ and $s^{o}_{i,cat,in}$ are entropy of substance at reference condition corresponding to anode and cathode inlet respectively, $E^{PH}_{ano,out}$ and $E^{PH}_{cat,out}$ are physical exergy at anode and cathode outlet respectively, $h_{i,ano,out}$ and $h_{i,cat,out}$ are enthalpy of substance at anode and cathode outlet respectively, $s_{i,ano,out}$ and $s_{i,cato,out}$ are entropy of substance at anode and cathode outlet respectively, $s^{o}_{i,ano,out}$ and $s^{o}_{i,cat,out}$ are entropy of substance at reference condition corresponding to anode and cathode outlet respectively, $E^{CH}_{cat,in}$ and $E^{CH}_{ano,in}$ are chemical exergy at anode and cathode inlet respectively, $E^{CH}_{ano,out}$ and $E^{CH}_{cat,out}$ are chemical exergy at anode and cathode outlet respectively, $\dot{E}_{xd}$ is exergy destruction in fuel cell, T_0 is temperature at reference condition in K, V_{cell} is actual cell voltage and I is current.

This chapter deals with the modeling of the basic components of the gas turbine power plant system. All the components have been modeled using a control volume approach.

4.1 Compressor

To develop an analytical mathematical model for the analysis of compressor following assumptions has been taken into consideration:

1. A control volume enclosing the compressor is considered.
2. The control volume operates at steady state.
3. For air, the ideal-gas mixture principles are valid, and air is mixture of O_2, N_2, H_2O, and CO_2.
4. The compressor operates adiabatically.
5. Kinetic and potential energy effects are negligible.

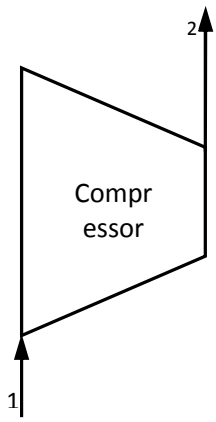

Figure 4.1: Control volume enclosing compressor

The function of the compressor is to raise the pressure of fluid from the inlet state 1 to the specified pressure at exit (state 2). The exit pressure is specified in terms of pressure ratio;

defined as the ratio of pressure of the fluid at exit to the pressure of the fluid at inlet. Mathematically:

$$p_{rc} = \frac{p_2}{p_1} \tag{4.1}$$

Where, p_{rc} is the compression pressure ratio, p_2 is the pressure of the fluid at exit of the compressor, and p_1 is the pressure of the fluid at inlet of the compressor. The pressure ratio expression is used to determine the pressure p_2.

To compress (i.e. to increase the pressure of) the air, energy is absorbed by the compressor in the form of work. The specific work required to compress the air is given as:

$$w_{com} = (h_2 - h_1)/\eta_{com,mech} \tag{4.2}$$

Where, $w_{com}$is the specific work done on the compressor, h_2 is the actual specific enthalpy of the fluid at compressor outlet, h_1 is the specific enthalpy of the fluid at compressor inlet, and $\eta_{com,mech}$is the mechanical efficiency of the compressor. The enthalpy of the fluid at compressor inlet is calculated by knowing the pressure and temperature of the fluid at compressor inlet i.e. p_1 and T_1 respectively. Here its worth to note that eq. (4.2) is written without considering the sign convention. The actual specific enthalpy at outlet (h_2) of the compressor is calculated from the expression of the isentropic efficiency given as:

$$\eta_{com,is} = \frac{h_{2s} - h_1}{h_2 - h_1} \tag{4.3}$$

Where, in eq. (4.3) $\eta_{com,is}$ the isentropic efficiency of the compressor and $h_{2s}$is the specific enthalpy at the outlet of the compressor for an isentropic compression. Since for an isentropic compression the entropy change is zero, for the isentropic compression of an ideal-gas mixture we can write:

$$s_{2s} - s_1 = x_{1N_2}\left[s^o(T_{2s}) - s^o(T_1) - R_u ln\frac{p_2}{p_1}\right]_{N_2} + x_{1O_2}\left[s^o(T_{2s}) - s^o(T_1) - R_u ln\frac{p_2}{p_1}\right]_{O_2} + x_{1CO_2}\left[s^o(T_{2s}) - s^o(T_1) - R_u ln\frac{p_2}{p_1}\right]_{CO_2} + x_{1H_2O}\left[s^o(T_{2s}) - s^o(T_1) - R_u ln\frac{p_2}{p_1}\right]_{H_2O} = 0 \quad (4.4)$$

Where, s_{2s} is specific entropy of the mixture after isentropic compression, s_1 is the specific entropy of the mixture at inlet of the compressor, T_1 and T_{2s} are temperature of the fluid at inlet and after isentropic compression respectively, x_{1i} is the mole fraction of the gases where i denotes the type of species present in the mixture, and s^o is the specific entropy at reference pressure (p_{ref} taken as 1 bar) and at corresponding temperature. Now, by evaluating specific entropies at T_1 and inserting the specific entropy expression for the species in eq. (4.4), then the solution of equation gives the value of T_{2s}. By knowing the T_{2s} the corresponding enthalpy of the mixture can be evaluated by using ideal-gas mixture principle.

The exergy balance equation for compressor can be written as:

$$E_1 + W_T = E_2 + E_d \quad (4.5)$$

Where, E_1 and E_2 are exergy of substance at inlet and outlet of compressor respectively, E_d and W_c is exergy destruction in compressor and work input to the compressor respectively.

4.2 Combustion chamber

To develop an analytical mathematical model for the analysis of combustion chamber following assumptions has been taken into consideration:

1. A control volume enclosing the combustion chamber is considered.

2. The control volume operates at steady state.
3. For air and combustion products, the ideal-gas mixture principles are valid.
4. The combustion is complete, N_2 is inert.
5. Kinetic and potential energy effects are negligible.
6. Heat transfer from the control volume is 2% of the lower heating value (LHV) of the fuel.

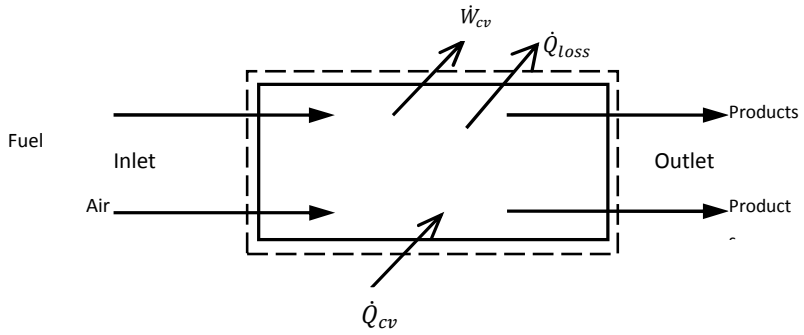

Figure 4.2: Control volume enclosing combustion chamber

Let, λ is fuel-air ratio on molar basis. The molar rate flow of the fuel, air, and combustion products are related as follows:

$$\lambda = \frac{\dot{n}_F}{\dot{n}_a}, \qquad 1 + \lambda = \frac{\dot{n}_P}{\dot{n}_a} \tag{4.6}$$

Where, $\dot{n}_F$, $\dot{n}_a$ and $\dot{n}_P$ are the molar flow rate of fuel, air, and combustion products respectively. Applying first law of thermodynamics to the control volume:

$$\sum \dot{n}_i\, h_i + \dot{Q}_{cv} - \dot{Q}_{loss} - \dot{W}_{cv} = \sum \dot{n}_e\, h_e \tag{4.7}$$

By knowing the inlet enthalpy and lower heating value of the fuel enthalpy at outlet can be calculated and outlet temperature can be evaluated through iterative method.

The exergy balance equation for combustion chamber is given as:

$$E_1 = E_2 + E_d \tag{4.8}$$

Where, E_1 and E_2 are exergy of substance at inlet and outlet of combustion chamber respectively, and E_d is exergy destruction in combustion chamber.

4.3 Turbine

To develop an analytical mathematical model for the analysis of gas turbine following assumptions has been taken into consideration:

1. A control volume enclosing the gas turbine is considered.
2. The control volume operates at steady state.
3. For combustion products, available at gas turbine inlet, the ideal-gas mixture principles are valid.
4. Kinetic and potential energy effects are negligible.
5. Heat transfer from the control volume is negligible.

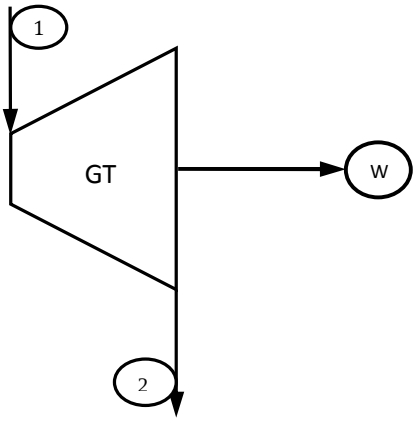

Figure 4.3: Gas turbine

The function of turbine is to produce power by expansion of fluid at high pressure and high temperature to lower pressure and lower temperature. The working fluid expands in the turbine from the inlet state 1 to the specified pressure at exit (state 2). The exit pressure is specified in terms of pressure ratio; defined as the ratio of pressure of the fluid at exit to the pressure of the fluid at inlet. Mathematically:

$$p_{re} = \frac{p_2}{p_1} \tag{4.9}$$

Where, p_{re} is the expansion pressure ratio, p_2 is the pressure of the fluid at exit of the compressor, and p_1 is the pressure of the fluid at inlet of the compressor. The pressure ratio expression is used to determine the pressure p_2.

Due to expansion of working fluid work transfer takes place, the specific work produced by the turbine is determined from enthalpy change of the working fluid. Mathematically, it is given as:

$$w_{tur} = (h_1 - h_2)/\eta_{tur,mech} \tag{4.10}$$

Where, w_{tur} is the specific work delivered by the turbine, h_1 is the specific enthalpy of the fluid at turbine inlet, h_2 is the actual specific enthalpy of the fluid at turbine outlet, and $\eta_{tur,mech}$ is the mechanical efficiency of the turbine. The enthalpy of the fluid at turbine inlet is taken same as the enthalpy at combustion chamber exit. The actual specific enthalpy at outlet (h_2) of the turbine is calculated from the expression of the isentropic efficiency given as:

$$\eta_{tur,is} = \frac{h_1 - h_2}{h_1 - h_{2s}} \tag{4.11}$$

Where, in eq. (4.11) h_{2s} is the specific enthalpy at the outlet of the turbine for an isentropic expansion. Since for an isentropic expansion the entropy change is zero, for the isentropic expansion of an ideal-gas mixture we can write:

$$s_{2s}(T_{2s}, p_2) - s_1(T_1, p_1) = 0 \tag{4.12}$$

Where, s_{2s} is specific entropy of the mixture after isentropic expansion, s_1 is the specific entropy of the mixture at inlet of the turbine, T_1 and T_{2s} are temperature of the fluid at inlet and after isentropic expansion respectively, solving equation (4.12) gives the value of T_{2s}. By knowing the T_{2s} the corresponding enthalpy of the working fluid (gas mixture) can be evaluated by using ideal-gas mixture principle. The exergy balance equation for gas turbine can be written as:

$$E_1 = W_T + E_2 + E_d \tag{4.13}$$

Where, E_1 and E_2 are exergy of substance at inlet and outlet of gas turbine respectively, E_d and W_T is exergy destruction in gas turbine and work delivered by the turbine respectively.

4.4 Recuperator

Heat exchanger/Recuperator is a device in which heat is transferred between two moving fluids.

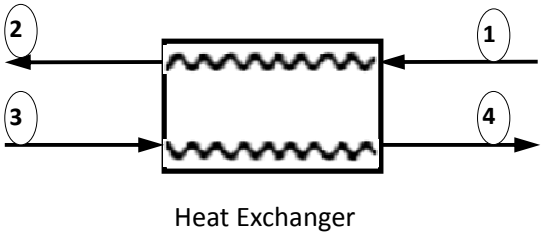

Figure 4.4 Control Volume for Heat Exchanger

The effectiveness of the recuperator is described as:

$$\epsilon = \frac{T_4 - T_3}{T_1 - T_3} \tag{4.14}$$

Writing the energy balance equation for the recuperator control volume one may find the outlet temperature or enthalpy depending upon the formulation:

$$(h_4 - h_3) = (h_1 - h_2) \tag{4.15}$$

Where, T_3, T_4, h_3, and h_4 are temperature and specific enthalpy of cold stream at inlet and outlet respectively; T_1 , T_2, h_1, and h_2 are temperature and specific enthalpy of hot stream at inlet and outlet respectively. The exergy balance equation for heat exchanger can be written as:

$$E_1 + E_3 = E_2 + E_4 + E_d \tag{4.16}$$

Where, E_1 and E_3 are exergy of hot and cold stream at inlet of heat exchanger, E_2 and E_4 are exergy of hot and cold stream at outlet of heat exchanger and E_d is exergy destruction in heat exchanger.

Chapter 5

Hybrid System

This chapter explains the working of the hybrid system and the different techniques used in the hybrid system. As in introduction it is said that Hybrid system couples the micro gas turbine with the fuel cell (generally SOFC), there are some methods to couple them. These methods will be discussed here in detail after an introduction about hybrid system.

5.1 Hybrid System

Hybrid Systems are power generation systems in which a heat engine, such as a gas turbine, is combined with a non-heat-engine, such as a fuel cell. The resulting system exhibits a synergism in which the combination performs with an efficiency that far exceeds that which can be provided by either system alone. Thus the combination performs better than the sum of its parts. The working definition of Hybrid Power Systems is evolving, but currently the following statement captures the basic elements:

Hybrid Power Systems combine two or more energy conversion devices that, when integrated provide (1) additional advantages over those devices operated individually, and (2) a synergism that yields performance that exceeds the sum of the components. With these attributes, combined with an inherent low level of pollutant emission, Hybrid configurations are likely to represent a major percentage of the next generation advanced power generation systems [59]. Studies on plant concepts for SOFC/GT-systems attract more attentions recently. A hybrid system consisting of a micro turbine and a SOFC achieves electrical efficiencies that are comparable to those of large power plants and beyond, especially in the case of direct integration and high SOFC-operating temperatures and turbine inlet temperatures.

A MGT has a smaller volume and weight but also a lower efficiency (about 30%) and larger emissions than a "normal" gas turbine. Therefore, a MGT working as a stand-alone device generates not so much benefit. A fuel cell is a clean energy generator and has a considerably higher and constant efficiency even at different operating temperatures, but its volume is still

extremely large. Normally, the fuel cell is a SOFC (solid oxide fuel cell) which works at temperatures of about 950°C, so that the temperature level of the exhaust heat is high enough to be used for the operation of a micro turbine. At the same time the exhaust heat of the turbine can be utilized in the fuel cell for the preheating of cathode- and anode-gas. The fuel utilization of solid oxide fuel cells lies in the range of 80% to 85%.

Therefore, a further enhancement of the efficiency is possible by an additional combustion of the fuel cell exhaust in the combustion chamber of the turbine. This means that hybrid MGT/FC systems could be a promising technology for distributed power supply.

5.2 Types of Hybrid System

There can be various plant layouts for a hybrid system combining solid oxide fuel cell and gas turbine system but a simple classification of hybrid system can be made on the basis of coupling of the fuel cell with the micro gas turbine. On the basis of coupling scheme or integration scheme, there are two types of hybrid system:

1. Integration of MGT and SOFC via Heat Exchanger or indirect fuel cell turbine cycle

2. Direct Integration of MGT and SOFC or direct fuel cell cycle

5.2.1 Integration of MGT and SOFC via Heat Exchanger or indirect fuel cell turbine cycle

The simplest fuel cell/gas turbine cycle consists of a coupling of the two components by a heat exchanger. In this case the fuel cell exhaust heats compressed air in the micro gas turbine recuperator (Figure 5.1) while anode and cathode gas preheating is done with heat from the gas turbine exhaust gas and the heat released from combustion of residual fuel contained in the fuel cell exhaust gas.

As this concept leads to high temperatures at the recuperator exit, there is only small additional firing necessary to reach the nominal turbine inlet temperature, provided this is in the same range as the temperature of operation of the fuel cell. The high temperatures that occur in the recuperator require special materials, however, particularly high temperature alloys or expensive

ceramics. There is still the need to develop inexpensive and heat-resistant materials, resulting in components with a sufficient life-span. The same problem occurs at the interconnection between SOFC and recuperator.

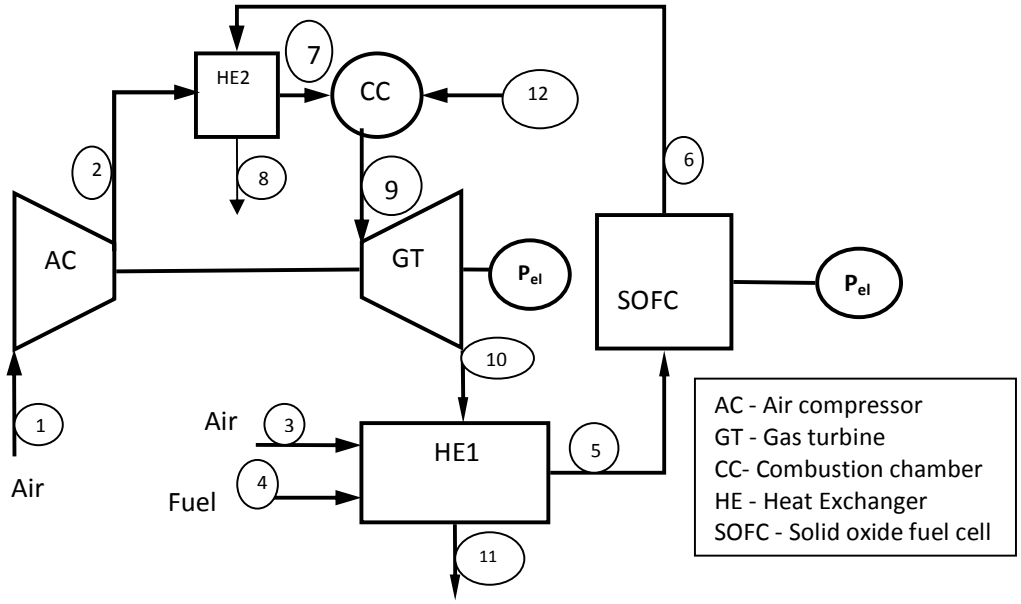

Figure 5.1: Integration of a Micro Turbine and a SOFC by a Heat Exchanger

The various state points shown in the Fig.5.1 are as follows:

State 1: Inlet to air compressor,

State 2: Outlet from air compressor and inlet to heat exchanger,

State 3: Air entering into heat exchanger 1 at atmospheric pressure,

State 4: Fuel entering into heat exchanger 1 at atmospheric pressure,

State 5: Gases leaving the heat exchanger 1 and entering into fuel cell,

State 6: Gases leaving the fuel cell and entering into another heat exchanger 2,

State 7: Compressed air leaving the heat exchanger 2 and entering into combustion chamber,

State 8: Mixture of gases leaving the heat exchanger 2 and entering into atmosphere,

State 9: Mixture of gases at combustion chamber exit and at turbine inlet,

State 10: Mixture of gases at turbine exit entering into heat exchanger 1,

State 11: Mixture of gases leaving the heat exchanger 1 and entering into atmosphere,

State 11: Fuel supply into combustion to achieve the desired turbine inlet temperature (TIT).

An additional problem in this area is the necessity for adapting the cooling system of the combustion chamber walls to the elevated temperatures of the entering gas. Often the combustion chamber is kept in operation after the introduction of the fuel cell exhaust gas into the process. This is done in order to reach the maximum turbine inlet temperature. But then the film cooling of the combustion chamber walls has to be modified in such a way that the admissible material temperatures are met. Otherwise, also in this area new materials have to be applied. Another possibility is to omit additional combustion and to accept lower turbine inlet temperatures.

5.2.2 Direct Integration of MGT and SOFC

An alternative to combining a fuel cell and a micro gas turbine is the direct integration of the two components. This configuration is more popular than indirect integration system. If this is the case, the SOFC can be operated at higher pressure which is beneficial for its efficiency, and exegetic losses at heat exchangers are reduced.

This configuration offers an electrical efficiency of 50% to 60% assuming a conventional turbine inlet temperature and an SOFC operating temperature range of 900 - 1000°C This result is in agreement with other studies based on state-of-the-art technology. The plant concept for this configuration is shown in Fig. 5.2.

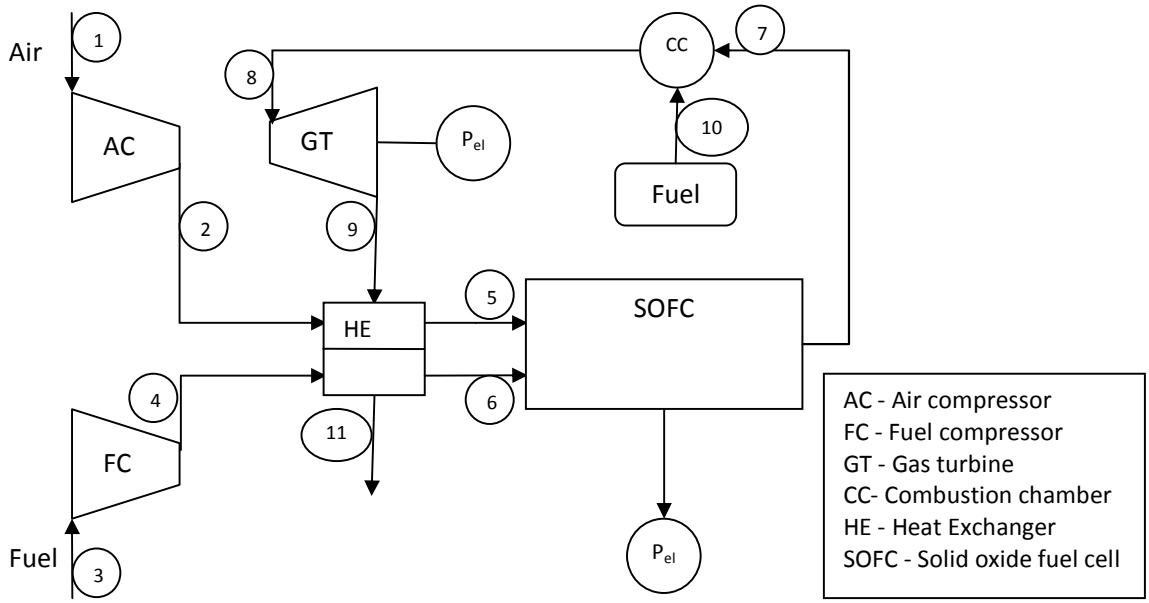

Figure 5.2: Direct Integration of a Micro Turbine and a SOFC

The various state points shown in Fig. 5.2 are as follows:

State 1: Inlet to air compressor,

State 2: Outlet from air compressor and inlet to heat exchanger,

State 3: Inlet to fuel compressor,

State 4: Outlet from fuel compressor and inlet to heat exchanger,

State 5: Air leaving the heat exchanger and entering into fuel cell,

State 6: Fuel leaving the heat exchanger and entering into fuel cell,

State 7: Mixture of gases at fuel cell exit entering into combustion chamber,

State 8: Mixture of gases at combustion chamber exit entering into gas turbine,

State 9: Mixture of gases at turbine exit entering into heat exchanger,

State 9: Mixture of gases at heat exchanger exit entering into atmosphere.

The fuel cell exhaust gas still contains 15% to 20% of the original fuel as residual combustible substances. These can be utilized for further temperature augmentation before the hot gases are expanded in the micro gas turbine yielding a temperature gain of 150 to 350 Kelvin at reference point operation (TSOFC = 950 °C, p_r=6,5). This operating point represents the basic condition on which further parameter variations of design point operating parameters are based. Compared to the original concept, where residual fuel is burnt for additional internal cathode/anode gas preheating, this alternative design requires increased internal anode and cathode gas recirculation for temperature equalization.

For all scenarios assuming additional firing in the gas turbine combustor, efficiency increases with pressure. The reason for this behavior is that a larger portion of the fuel is added in the fuel cell rather than in the gas turbine combustor. This is reflected by an increase of temperature augmentation by residual fuel combustion compared to the above mentioned basic condition. It leads to a better fuel utilization at given turbine inlet temperatures. The addition of conventional fuel should be limited to a minimum amount, in order to maximize the efficiency gain. This requires appropriate burner systems which avoid flash-back and ensure stable premixed combustion with a low amount of auxiliary fuel.

5.3 Applications of Hybrid System

Hybrid system can be applied in the residential area as well as in small industry, trade and services or public buildings as they offer an opportunity for an environmentally friendly electricity supply and, at the same time, a cooling and heat supply with high fuel utilization. The world's first SOFC/gas turbine hybrid system was delivered to Southern California Edison for operation at the University of California, Irvine's National Fuel Cell Research Center. The hybrid system includes a pressurized SOFC module integrated with a micro turbine/generator supplied by Ingersoll-Rand Energy Systems (formerly Northern Research and Engineering Corp.). The system has a total output of 220 kW, with 200 kW from the SOFC and 20 from the micro turbine

generator. This system, a photograph of which is shown below, is the first-ever demonstration of the SOFC/gas turbine hybrid concept. This proof of concept demonstration is expected to demonstrate an electrical efficiency of ~55%. The system is being tested at the NFCRC to determine its operating characteristics and operating parameters. As of January 2002 the system has operated for 900+ hours and has demonstrated 53% electrical efficiency. It will be operated for several more months to gain experience for the design of prototypes and commercial products. Eventually, such SOFC/GT hybrids should be capable of electrical efficiencies of 60-70%.

6.1 Solution Methodology

First of all a hybrid system configuration was selected as shown in Figure 6.1. Then based upon the mathematical modelling presented in chapter 3 and 4, a computer program has developed. The computer program for the simulation of the model has been developed in the EES software. EES is a general equation solver with built-in functions for thermodynamic and transport properties. The diagram shown in Figure 6.1 has been also treated as information flow diagram for the system.

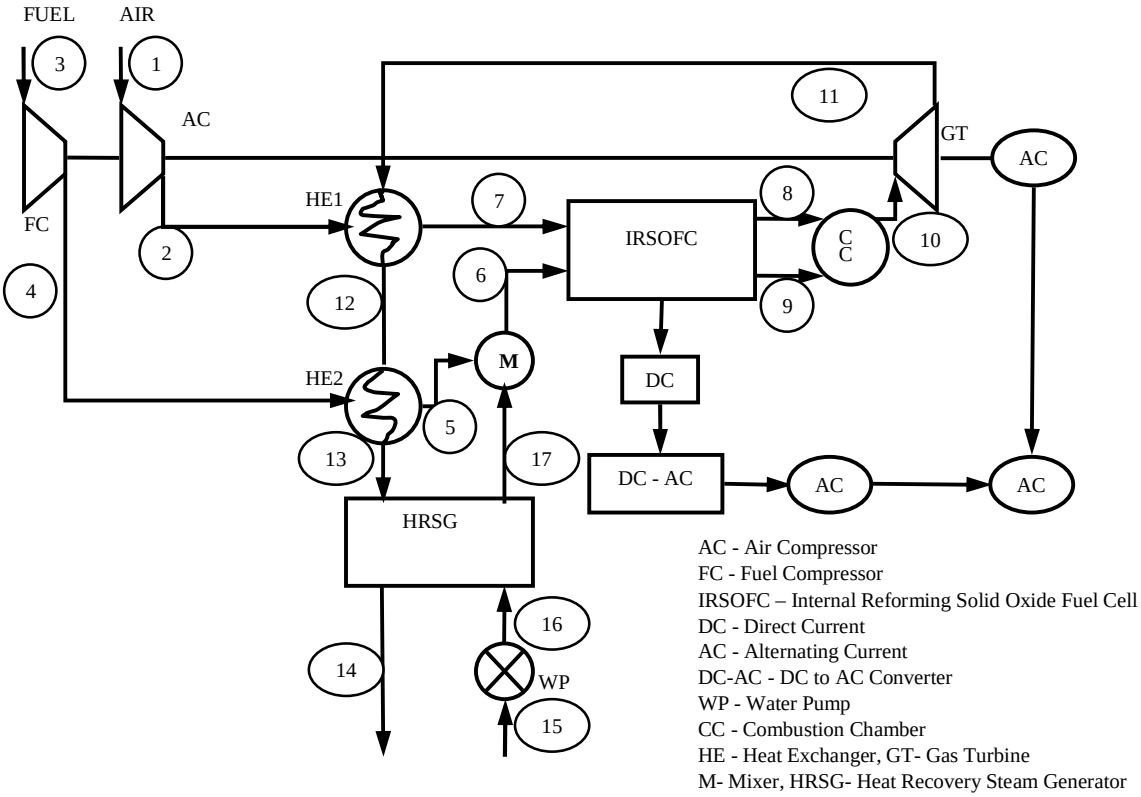

Figure 6.1: Hybrid System Configuration Considered for Analysis

The various state points of Fig. 6.1 are as follows:

State 1: Inlet to air compressor,

State 2: Outlet from air compressor and inlet to heat exchanger 1,

State 3: Inlet to fuel compressor fuel at atmospheric pressure enters into fuel compressor,

State 4: Fuel compressor outlet and compressed fuel enters into heat exchanger 2,

State 5: Fuel leaving heat exchanger 2 and entering into mixer,

State 6: Mixer outlet,

State 7: Compressed air leaving the heat exchanger 1 and entering into fuel cell,

State 8: Air at cathode outlet of the fuel cell,

State 9: Mixture of gases at anode outlet of the fuel cell,

State 10: Mixture of gases at turbine inlet leaving the combustion chamber,

State 11: Mixture of gases at turbine exit, leaving turbine after expansion,

State 12: Hot gases leaving the heat exchanger 1 and entering into heat exchanger 2,

State 13: Hot gases leaving the heat exchanger 2 and entering into heat recovery steam generator,

State 14: Hot gases leaving the heat recovery steam generator and entering into atmosphere,

State 15: Water enters into water pump i.e. inlet to water pump,

State 16: Water pump outlet, water leaving the water pump and compressed water entering into heat recovery steam generator.

State 17: Heat recovery steam generator outlet, steam leaving heat recovery steam generator and entering into mixer.

The information flow for combined hybrid system can be summarized as follows:

[1] At compressors and pump known inlet conditions are specified with pressure ratio, and compressor isentropic and mechanical efficiency.

[2] Heat exchanger and HRSG analysis requires effectiveness as an input and outlet conditions of streams are determined.

[3] For calculation of properties of outlet stream equation for effectiveness and energy balance equation is solved simultaneously.

[4] The outlet temperature of the mixture of fuel and steam at mixer outlet is determined by assuming that total entropy change is zero.

[5] SOFC analysis requires all the geometric dimensions as an input for calculation of polarization losses. Chemical reactions are specified for calculation of heat generated and cell power.

[6] Combustion chamber analysis gets the input information from SOFC exit conditions. Input such as combustion chamber efficiency (η_{comb}), calorific value of fuel is supplied, based upon these inputs and assuming the complete combustion, the temperature and composition of outlet gas streams are determined.

[7] For calculation of temperature at combustion chamber exit, first of all composition of gases at outlet is determined by using stoichiometry equation then by using energy balance equation outlet temperature is calculated.

[8] For gas turbine outlet pressure is specified and power output is calculated.

[9] For calculation of chemical exergy the chemical exergy value at reference condition tabulated in Table 7.1 for various substances are supplied.

[10] Finally the program is executed and it calculates the value of desired parameters, such as cell voltage, turbine power output, first law efficiency, second law efficiency, exergy destruction in various component and properties of working fluid at different state points.

Table 6.1: Standard molar chemical exergy ex^{ch} (kJ/kmol) of various substances at 298.15 K and p_0 (1.013 bar) [60].

Substance	Formula	Model I	Model II
Nitrogen	$N_2(g)$	639	720
Oxygen	$O_2(g)$	3,951	3,970
Carbon dioxide	$CO_2(g)$	14,176	19,870
Water	$H_2O(g)$	8,636	9,500
Water	$H_2O(l)$	45	900
Carbon (graphite)	$C(s)$	404,589	410,260
Hydrogen	$H_2(g)$	235,249	236,100
Sulfur	$S(s)$	598,158	609,600
Carbon monoxide	$CO(g)$	269,412	275,100
Nitrogen monoxide	$NO(g)$	88,851	88,900
Sulfur dioxide	$SO_2(g)$	301,939	313,400
Nitrogen dioxide	$NO_2(g)$	55.565	55.600
Hydrogen peroxide	$H_2O_2(g)$	133,587	--------
Hydrogen sulfide	H_2S	799,890	812,000
Ammonia	$NH_3(g)$	336.684	337,900
Oxygen	$O(g)$	231,968	233,700
Hydrogen	$H(g)$	320,822	331,300
Nitrogen	$N(g)$	453,821	---------
Methane	$CH_4(g)$	824,348	831,650
Acetylene	$C_2H_2(g)$	----------	1,265,800
Ethylene	$C_2H_4(g)$	----------	1,361,100
Ethane	$C_2H_6(g)$	1,482,033	1,495,840
Propylene	$C_3H_6(g)$	----------	2,003,900
Propane	$C_3H_8(g)$	----------	2,154,000
n-Butane	$C_4H_{10}(g)$	----------	2,805,800
n-Pentane	$C_5H_{12}(g)$	----------	3,463,300
Benzene	$C_6H_6(g)$	----------	3,303,600
Octane	$C_8H_{18}(l)$	----------	5,413,100
Methanol	$CH_4OH(g)$	715,069	722,300
Methanol	$CH_4OH(l)$	710,747	718,000
Ethyl alcohol	$C_2H_5OH(g)$	1,348,328	1,363,900
Ethyl alcohol	$C_2H_5OH(l)$	1,342,086	1,375,700

6.2 Input Parameter

The input parameters are summarized in the Table 6.2.

Table 6.2: INPUT PARAMETERS

PARAMETER	VALUE
Gas–air heat exchanger effectiveness	0.80
Gas–air heat exchanger effectiveness	0.80
Gas–superheated steam heat exchanger eff.	0.80
Combustor efficiency	0.98
Electric generator efficiency	0.98
Inverter efficiency	0.95
Pump isentropic efficiency	0.80
Fuel compressor isentropic efficiency	0.80
Air compressor isentropic efficiency	0.80
Gas turbine isentropic efficiency	0.80
Fuel compressor mechanical efficiency	0.98
Air compressor mechanical efficiency	0.98
Pump mechanical efficiency	0.98
Gas turbine mechanical efficiency	0.98
Limiting current density (A/m^2)	9000
Methane inlet molar flow rate (kmol/s)	0.0028
Water inlet molar flow rate (kmol/s)	0.0057
Oxygen inlet molar flow rate (kmol/s)	0.0070
Cell operating pressure (bar)	7x1.013
Environment pressure (bar)	1.013
Environment temperature (^oC)	25
Fuel utilization factor	0.85
Minimum steam-to-carbon ratio	2.04
Cell current density (A/m^2)	1000
Anode thickness (cm)	0.010
Cathode thickness (cm)	0.220
Interconnection thickness (cm)	0.004
Cathode activation energy (kJ/kmol)	$1.1x10^5$
Anode activation energy (kJ/kmol)	$1.5x10^5$
γ_{anode} (A/m^2)	$2.13x10^8$
$\gamma_{cathode}$ (A/m^2)	$1.49x10^8$

Chapter 7

Result and Discussion

The formulation of fuel cell and gas turbine system is discussed in Chapter 3 and 4 respectively. The method of coupling gas turbine and fuel cell is also discussed in the chapter 5.Based upon these formulations and solution methodology discussed in chapter 6, results and discussions of the developed model are discussed below.

7.1 Program validation

The program has been validated for the calculated value of cell voltage and hybrid system electrical efficiency based upon the input parameter supplied. Since each and every data is not available in a single literature, various literatures have been considered for selection of input parameters for simulation of the developed model. The results obtained by the simulation are summarized in Table 7.1 and the value of various parameter obtained from execution of program is listed in Table 7.2.

Table 7.1: Result Validation

Component	Present model	Literatures
Cell voltage	0.67	0.683 [13] 0.684 [44]
Cell power output	1122	---------
Turbine power output	373.5 kW	----------
Total power output	1.495 MW	1.5 MW
First law electrical efficiency (LHV)	66.5%	60 % [48] 62.2%[41] 61.9% [44]
Second law efficiency	63.52%	----------

Table 7.2: Results obtained from calculation

State points	Molar flow (kmol/s)	Temperature (℃)	Pressure (bar)	Enthalpy (kJ/kmol)	Physical exergy (kJ/kmol)	Chemical exergy (kJ/kmol)
1	0.035	25	1.013	0	0	1301
2	0.035	296.3	7.093	8046	7161	1301
3	0.0028	25	1.013	-74595	0	824348
4	0.0028	209.4	7.093	-67091	6543	824348
5	0.0028	509.2	7.093	-50789	15109	824348
6	0.008512	485	7.093	23534	17048	276962
7	0.035	845.2	7.093	25655	18351	1301
8	0.03041	1073	7.093	33194	24096	901.5
9	0.01411	1073	7.093	-194441	29335	42985
10	0.04351	1407	7.093	-282255	35621	3360
11	0.04351	982.4	1.2	-44435	18435	3360
12	0.04351	584.2	1.2	-58599	8306	3360
13	0.04351	553.3	1.2	-59648	7628	3360
14	0.04351	318.5	1.2	-67367	3180	3360
15	0.005712	25	1.013	1889	0	45
16	0.005712	25.05	7.093	1903	10.98	45
17	0.005712	447.7	7.093	60702	19030	8636

7.2 Exergy Destruction

The exergy destruction in various components is tabulated in Table 7.2. From table 7.2 it can be very easily concluded that the maximum exergy destruction takes place in SOFC and in combustion chamber. This is due to chemical reaction in SOFC and combustion reaction in combustion chamber. Due to these reactions the compositions of substances are affected which results in maximum exergy destruction. The minimum exergy destruction is found in water pump

A comparative study of exergy destruction in each component with the help of bar chart is shown in Fig. 7.1.

Table 7.3: Exergy destruction in various components

Component	Exergy destruction (kW)
Air Compressor	36.71
Fuel Compressor	4.668
Heat Exchanger 1	49.11
Heat Exchanger 2	5.496
Mixer	5.893
Solid Oxide Fuel Cell	229.1
Gas Turbine	43.73
Heat Recovery Steam Generator	35.82
Combustion Chamber	84.5
Water Pump	0.06274

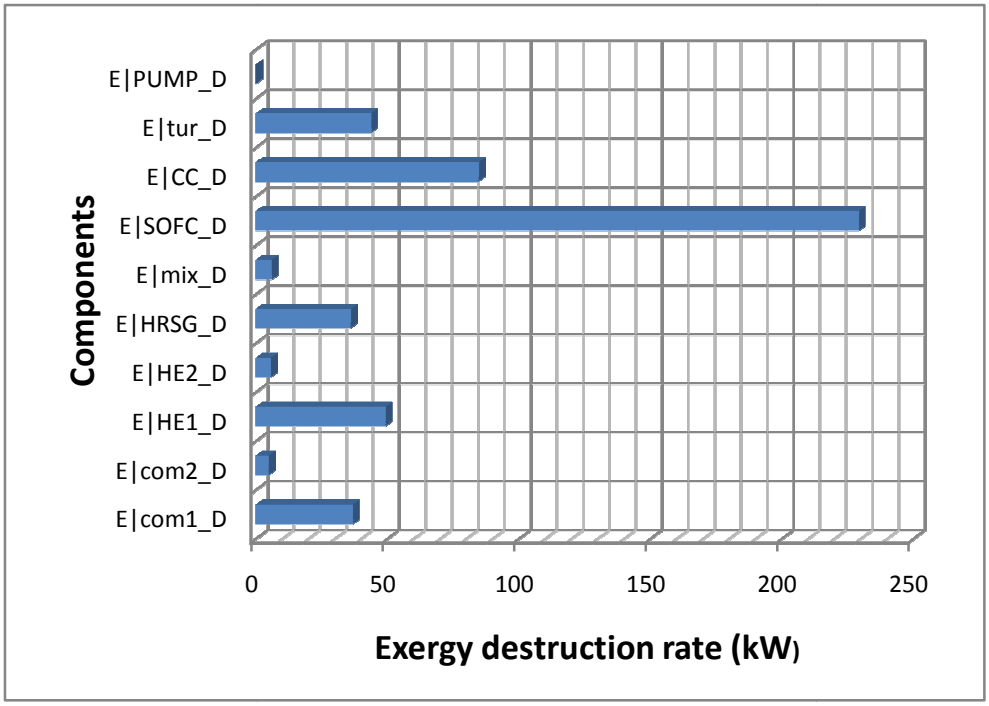

Figure 7.1 Exergy destruction rate in each component

7.3 Parametric Study

Based upon the important parameters of the present configuration of SOFC/GT hybrid system a detailed parametric study is presented here.

7.3.1 Effect of current density

The current density is very important parameter for evaluation of any fuel cell performance. Around 70% power output of the hybrid system is contributed by the SOFC unit and fuel cell power output is solely function of cell voltage, since cell current density affects the voltage of cell, it is very important to study the behavior of cell and its power output with respect to cell current density. In Fig. 7.2, the variation of cell activation loss vs. cell current density is shown.

The activation loss is predominant at low current density, it increases dramatically at low current density between 0 – 3000 A/m^2 and at higher current densities (more than 3000 A/m^2) the

variation is very less as compared to low current densities. Though it becomes constant at higher current density no decrease in the activation potential loss is registered.

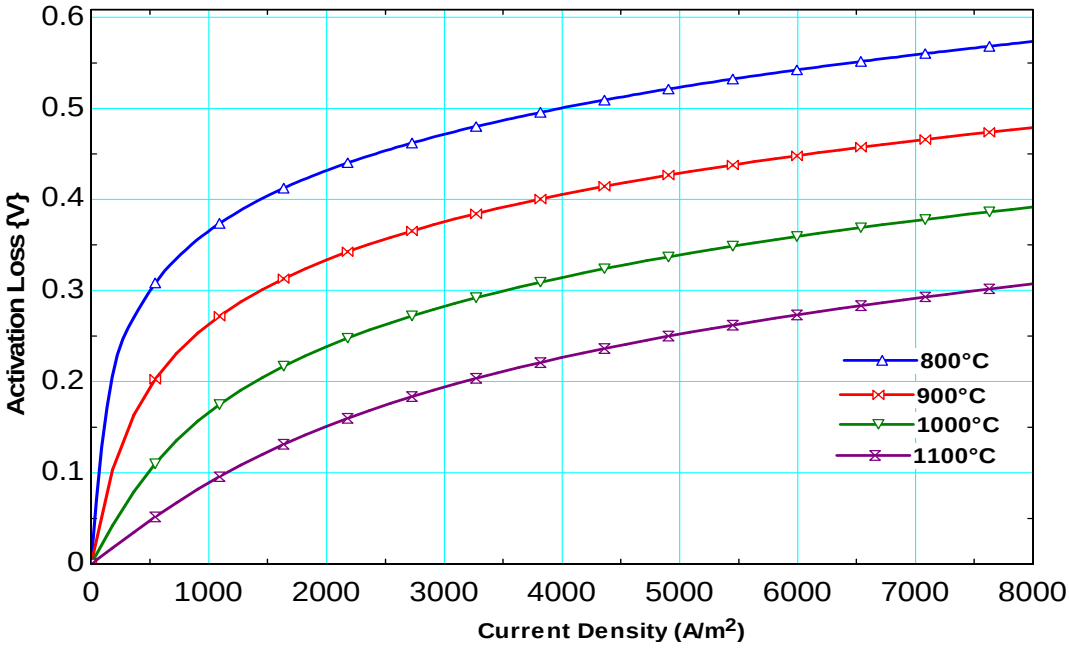

Figure 7.2: Activation loss vs. Current density (Present model)

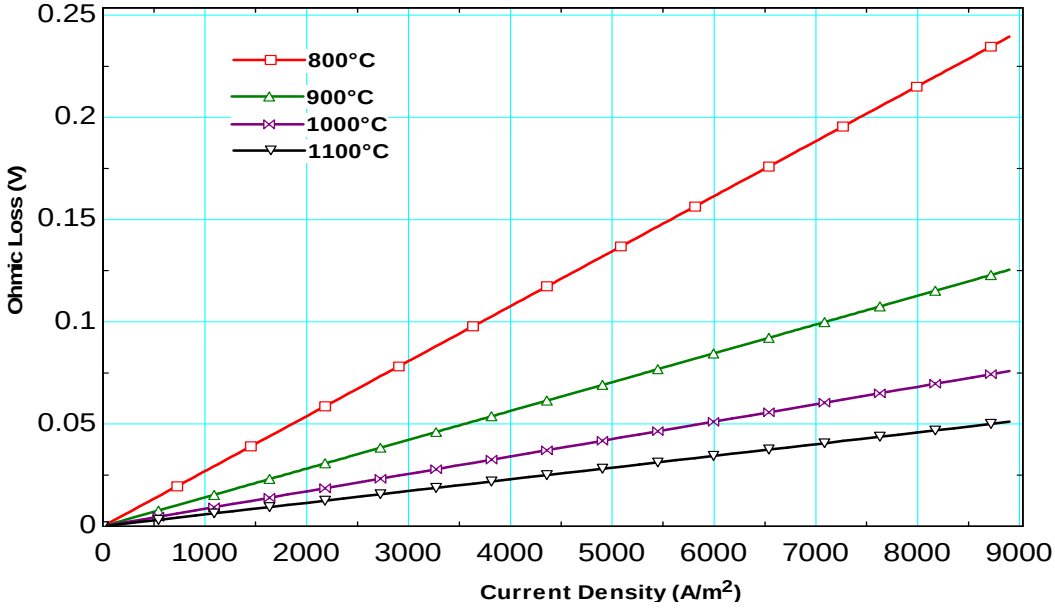

Figure 7.3: Ohmic loss vs. Current density (Present model)

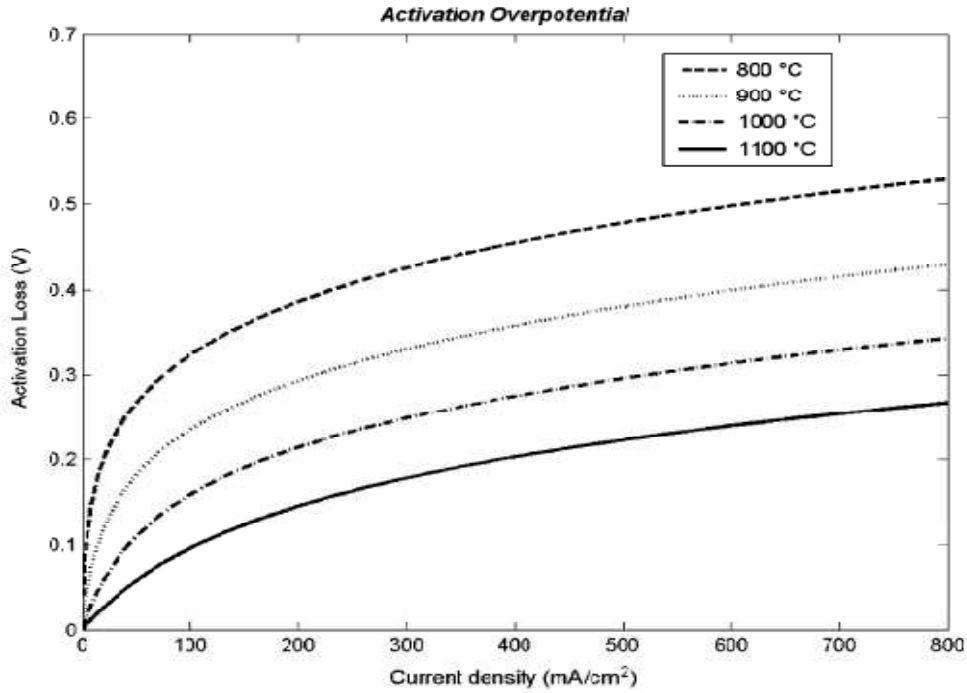

Figure 7.4: Activation loss vs. Current density (Literature) [48]

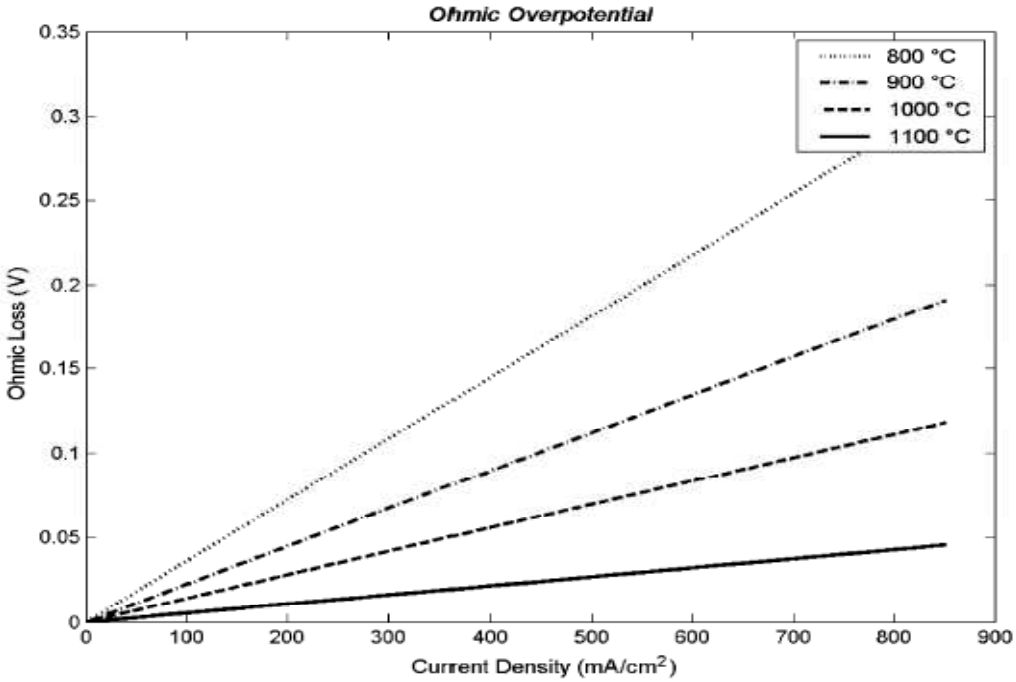

Figure 7.5: Ohmic loss vs. Current density (Literature) [48]

In Fig.7.3, effect of current density on Ohmic overpotential is shown; it follows a completely linear relationship nature with current density. It follows a linear relationship because the Ohmic overpotential is governed by the ohm's law. For a particular fuel cell it decreases or increases only when a change in current density is registered or operating temperature of cell changes since, resistivity as function of temperature is chosen. The results available in literature are shown in Fig 7.4 and 7.5 for effect of current density on activation and ohmic loss respectively.

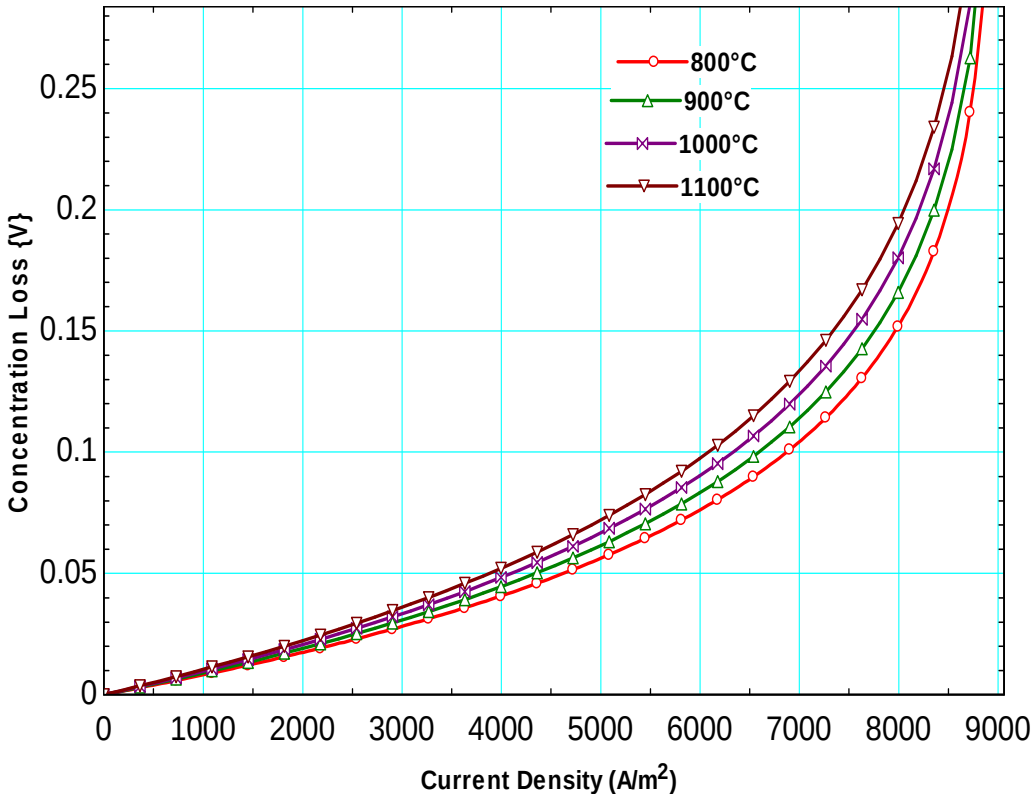

Figure 7.6: Concentration loss vs. Current density (Present model)

Effect of current density on concentration overpotential is shown in Fig. 7.6. The concentration overpotential is less dominant at low current density as compared to higher current density; it dramatically increases at higher current density. Generally at an optimum operating current density, decrease in cell voltage is around 0.05V due this concentration overpotential. As The cell operating temperature increases concentration polarization reduces but it has a very small effect on concentration overpotential.

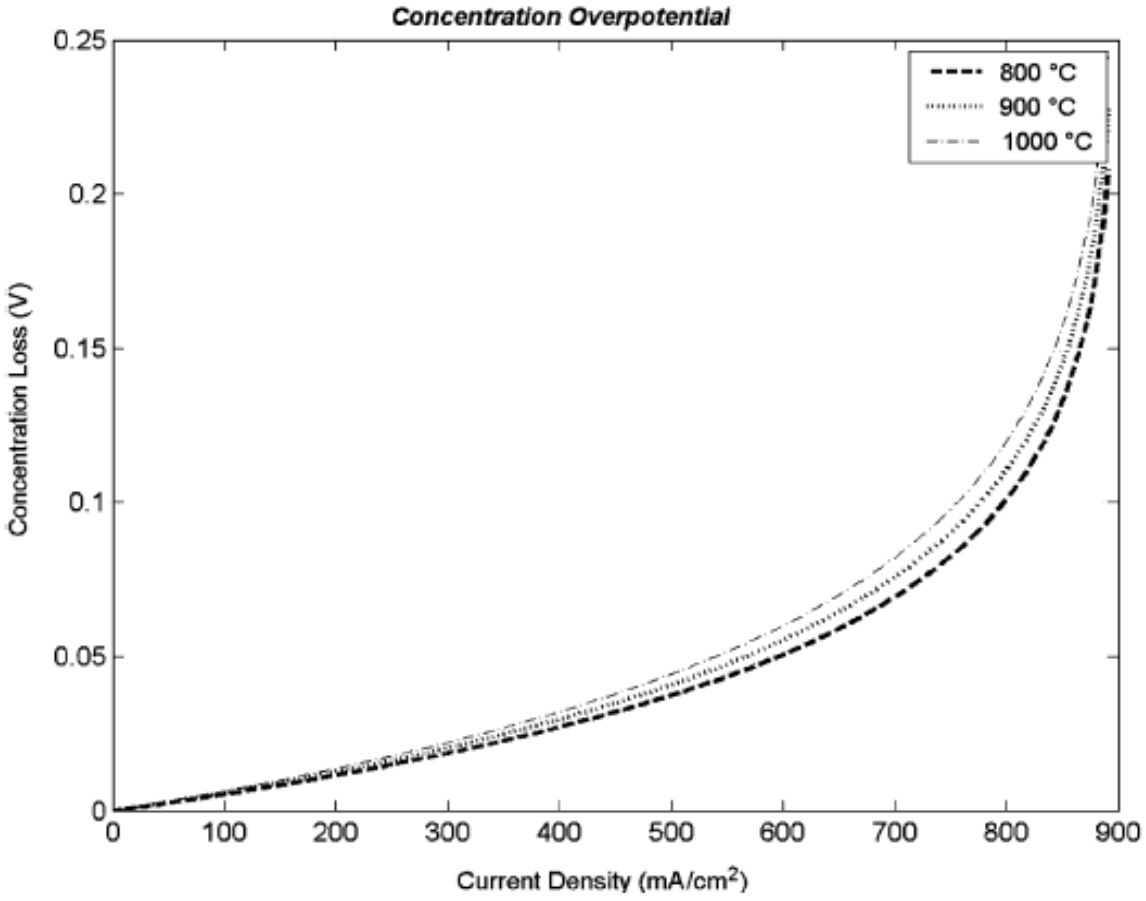

Figure 7.7: Concentration loss vs. Current density (Literature) [48]

Due to different overpotentials as discussed above, the actual cell voltage decreases from its theoretically calculated value. And since all the overpotentials are affected by current density, cell voltage also gets affected as the current density changes.

The variation of current density on cell voltage is shown in Fig. 7.8. The maximum cell voltage is at zero current density (also known as open circuit voltage); as the current density increases the overpotential becomes active and a decrease in voltage is registered. The entire performance of the fuel cell is governed by the current and voltage relationship. In the investigation it has been found that at low temperature voltage decreases rapidly with increase in current density as compared to higher operating cell temperature.

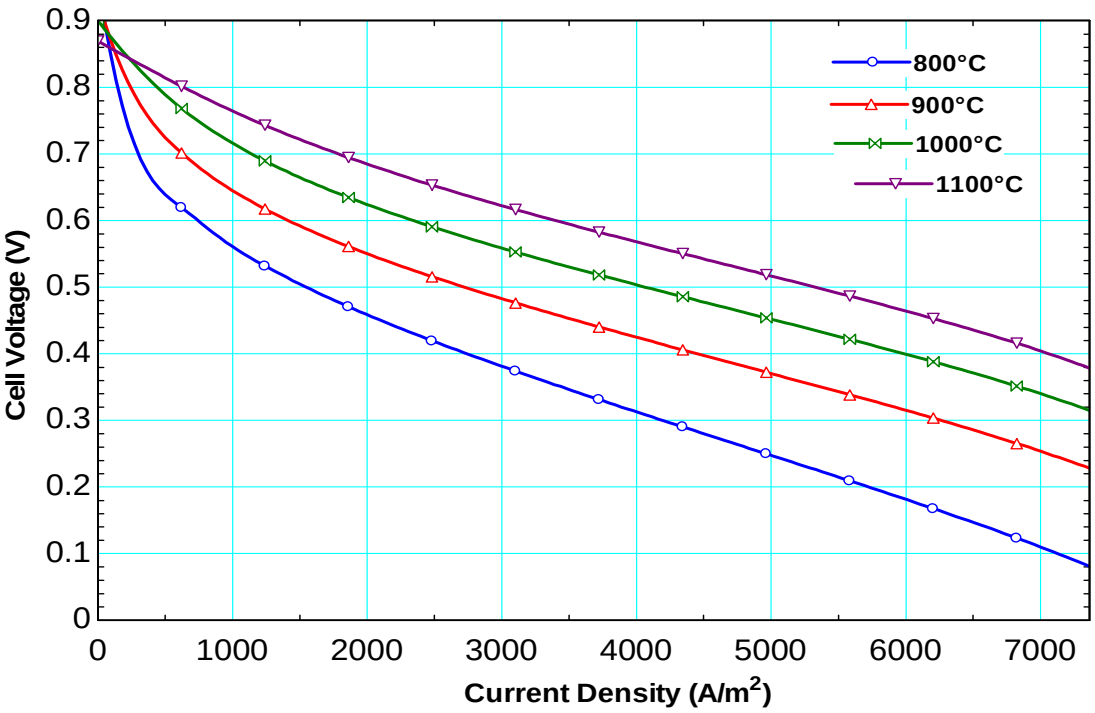

Figure 7.8: Cell voltage vs. Current density (Present model)

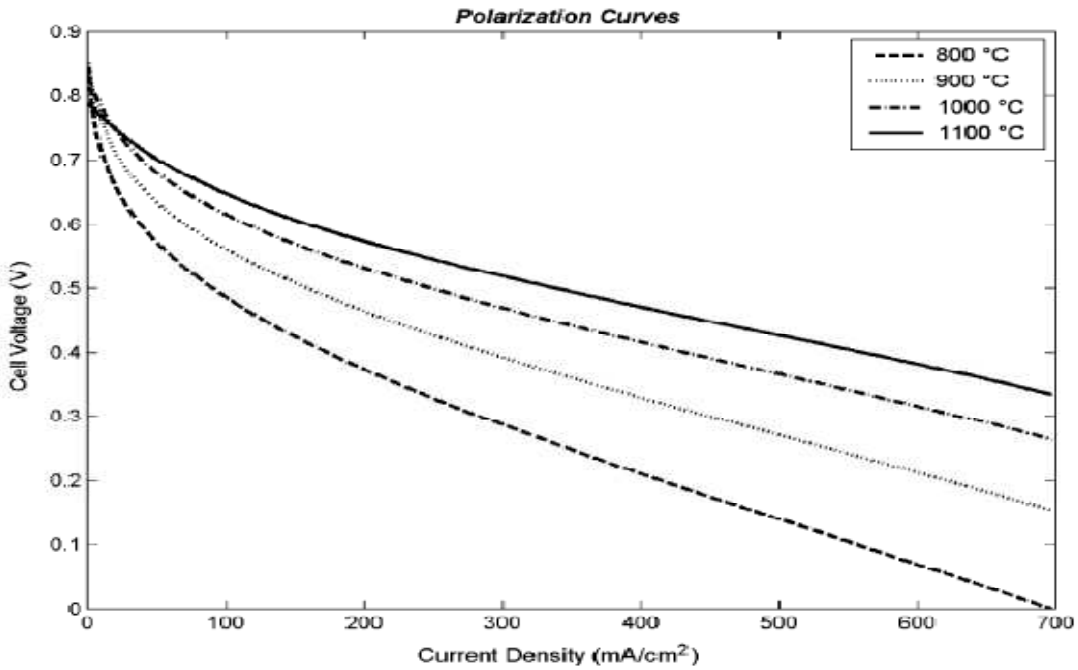

Figure 7.9: Cell voltage vs. Current density (Literature) [48]

Another very important parameter is cell power density. Effect of current density on this quantity is shown in Fig. 7.10.

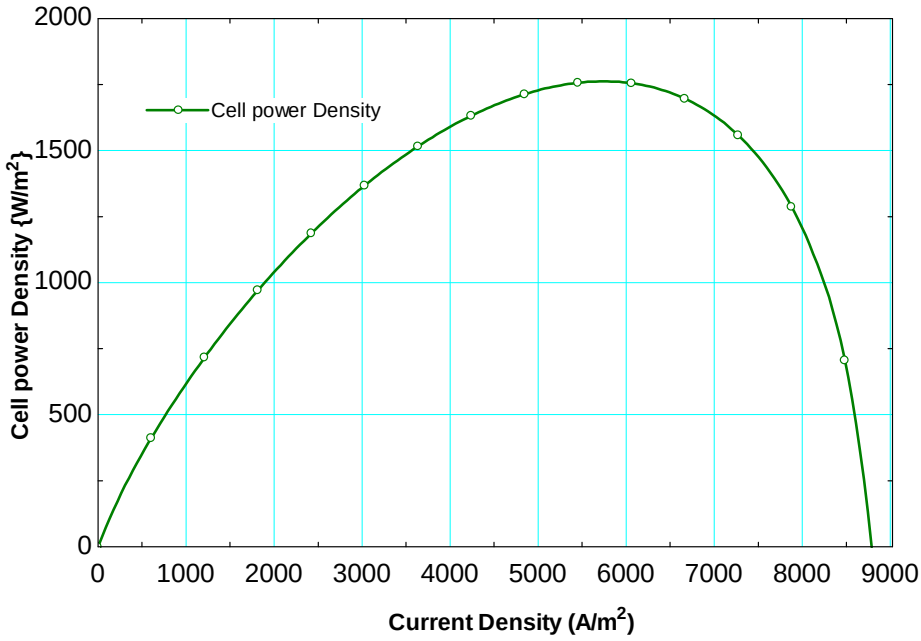

Figure 7.10: Cell power density vs. Current density (Present model)

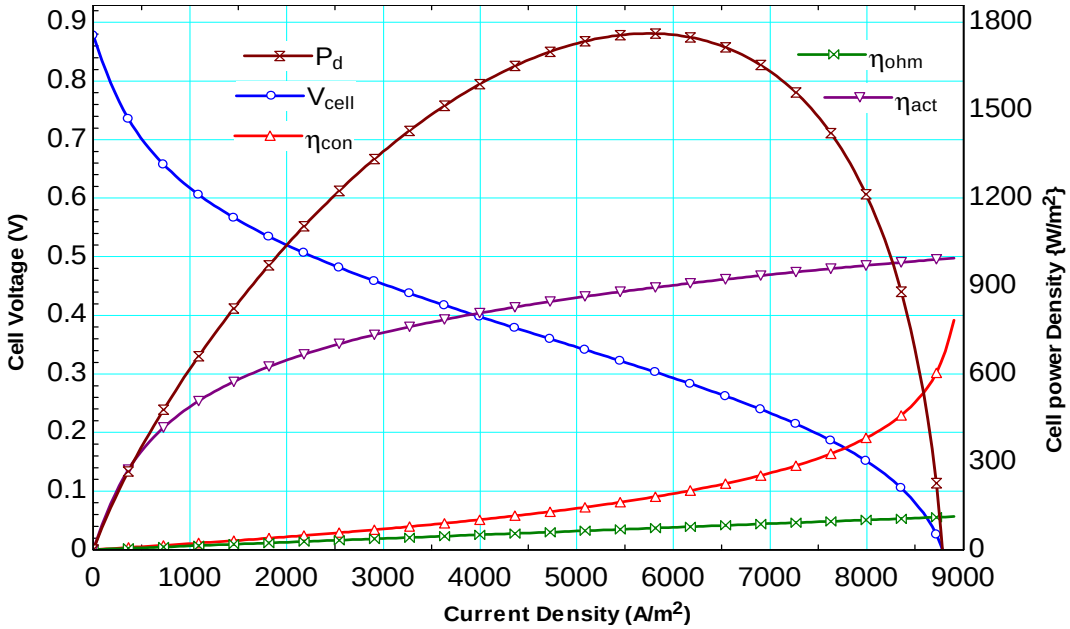

Figure 7.11: Effect of current density on various cell parameters (Present model)

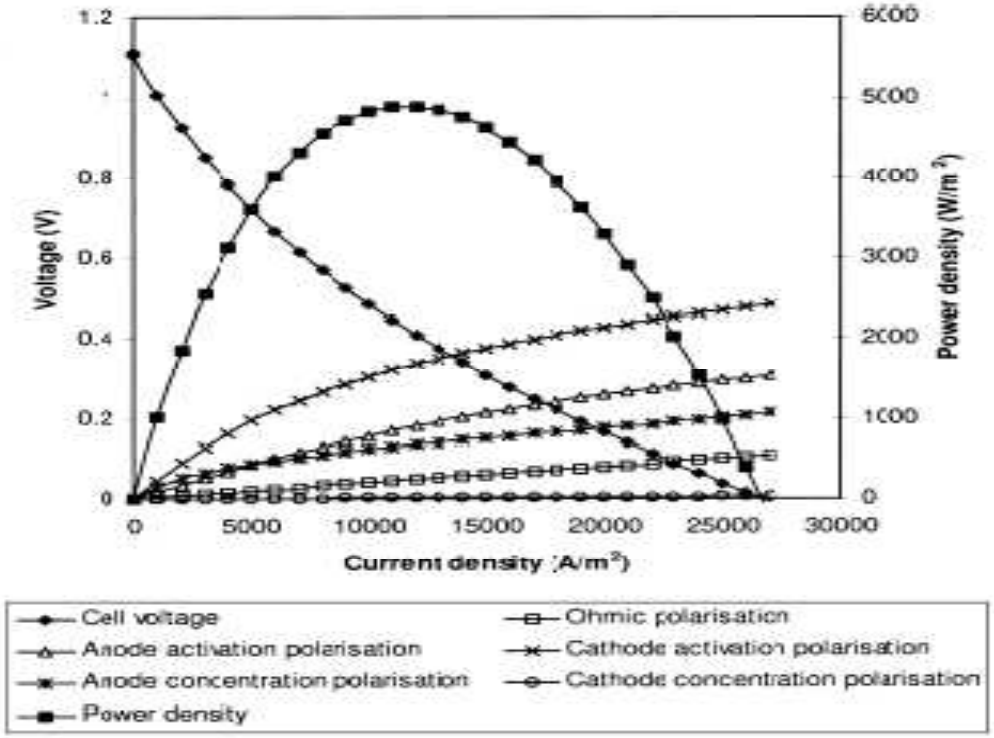

Figure 7.12: Effect of current density on various cell parameters (Literature) [61]

From Fig.7.10 it is clear that as power density increases, in similar fashion the power density decreases with varying current density. The maximum power density is somewhere at middle range of current density, but from Fig 7.10 and 7.11; it can be very easily concluded that though the power density is maximum between the current density 2000 to 3000 A/m^2 the optimum current density lies in between 1000 to 1500 A/m^2. In Fig. 7.11 the all the losses, cell voltage, and power density is combined in single graph for easier comparisons.

It is clear from above discussed results that voltage is highly influenced by the change in current density and as the power output is function of current and voltage, the current density will also affect the efficiency of the system. The effect of current density on electrical efficiency of the hybrid system is shown in Fig.7.13.

Efficiency decreases as the cell current density increases. This happens because most of the power output around 70% is due to SOFC and whose power output is solely the function of the

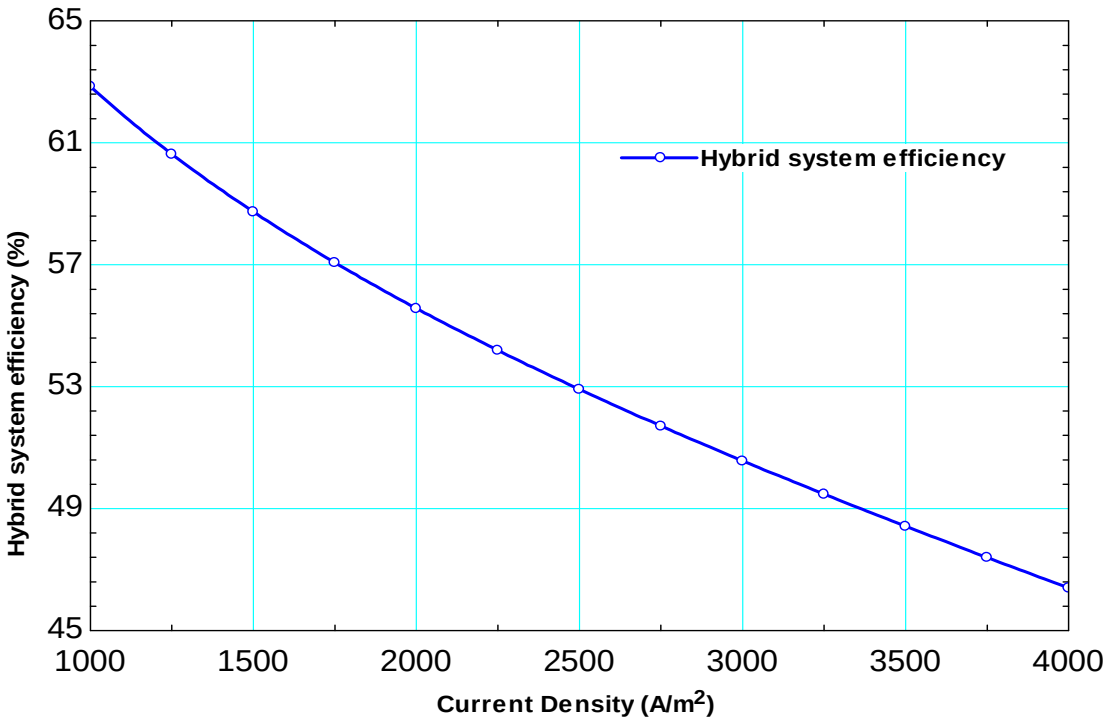

Figure 7.13: Hybrid system electrical efficiency vs. Current density (Present model)

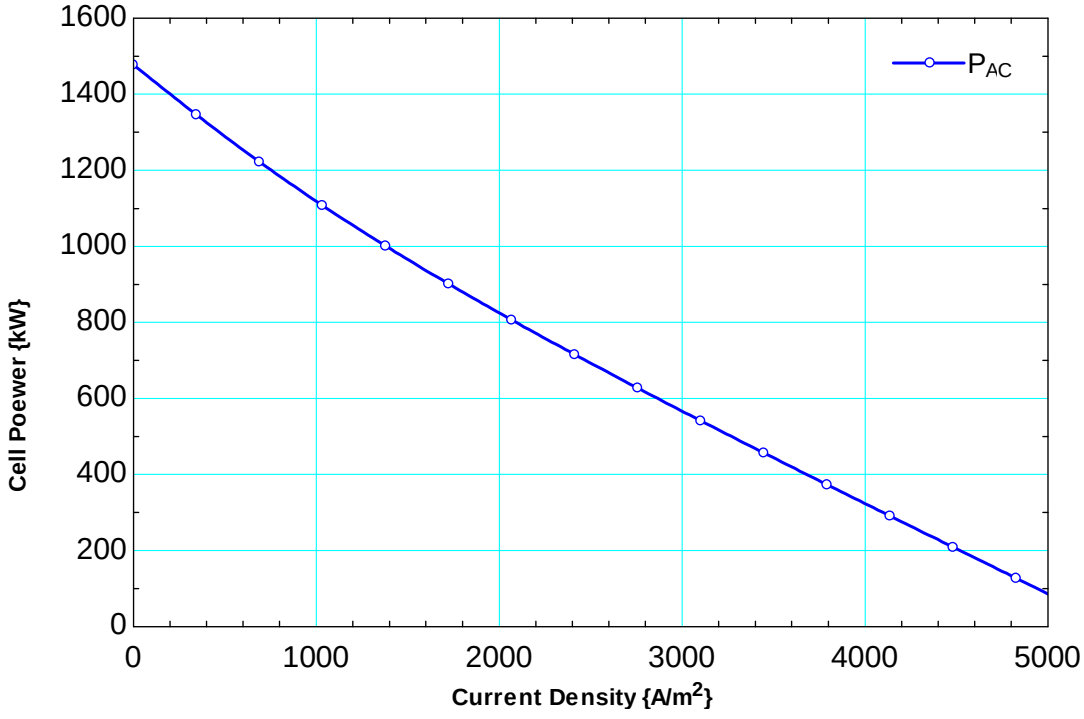

Figure 7.14: Cell Power vs. Current density (Present model)

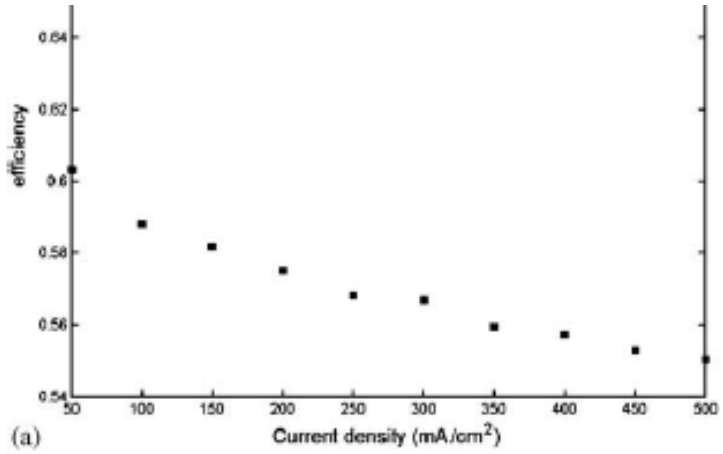

Figure 7.15: Hybrid system electrical efficiency vs. Current density (Literature) [48]

cell voltage and current. The efficiency reads a value around 30% while the cell contribution is very less, this because losses generate heat which is utilized by the GT system.

The variation of cell power output w.r.t. current density is also shown in Fig. 7.14. The cell power decreases as the current density increases and is reported minimum at 5000 A/m^2. The cell power decreases with increase in current density and at limiting current density, cell power output is zero because at limiting current density the value of cell voltage approaches to zero.

7.3.2 Effect of fuel flow

A variation of fuel flow between 0.0028 to 0.005 kmol/sec. and its effect on turbine power output and cell power output is shown in the Fig. 7.18 and 7.19 respectively. The cell power output increases from about 1200 to 1800 kW and turbine net power output varies in between 380 to 690 kW. In terms of percentage the effect of fuel flow is greater on turbine output as compared to cell power output.

The effect of fuel flow on cell power output and turbine output is shown in Fig. 7.16 and 7.17 respectively available in literature are in good agreements with the present model.

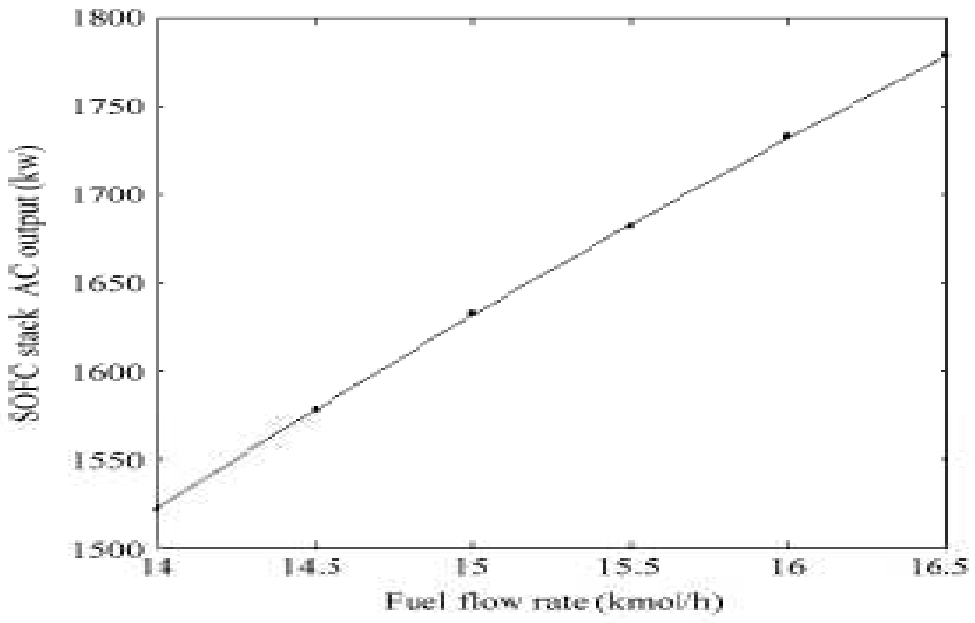

Figure 7.16: Cell work output vs. molar flow of fuel (Literature) [41]

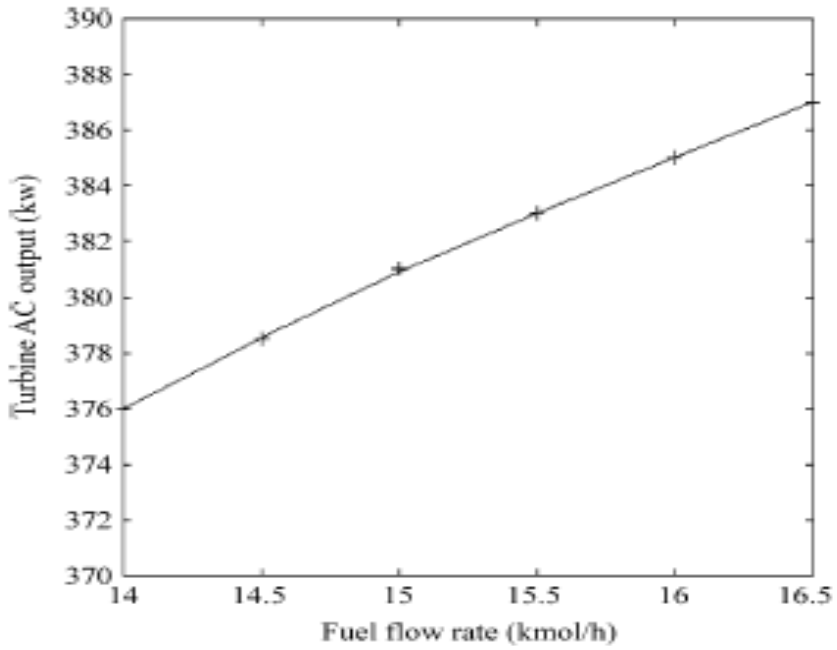

Figure 7.17: Turbine work output vs. molar flow of fuel (Literature) [41]

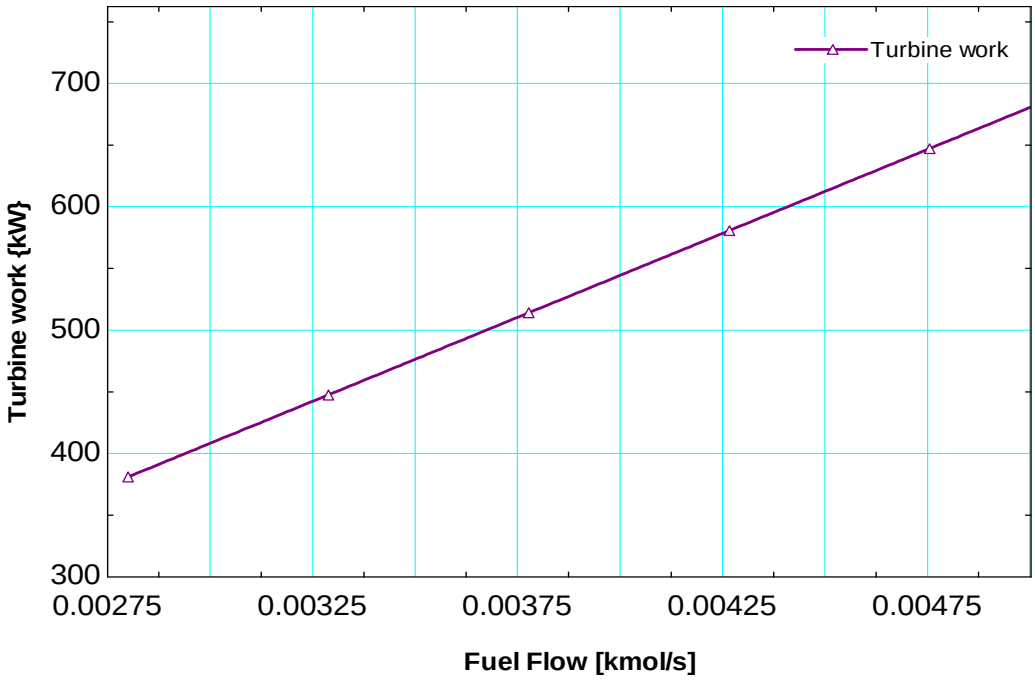

Figure 7.18: Turbine work output vs. molar flow of fuel (Present model)

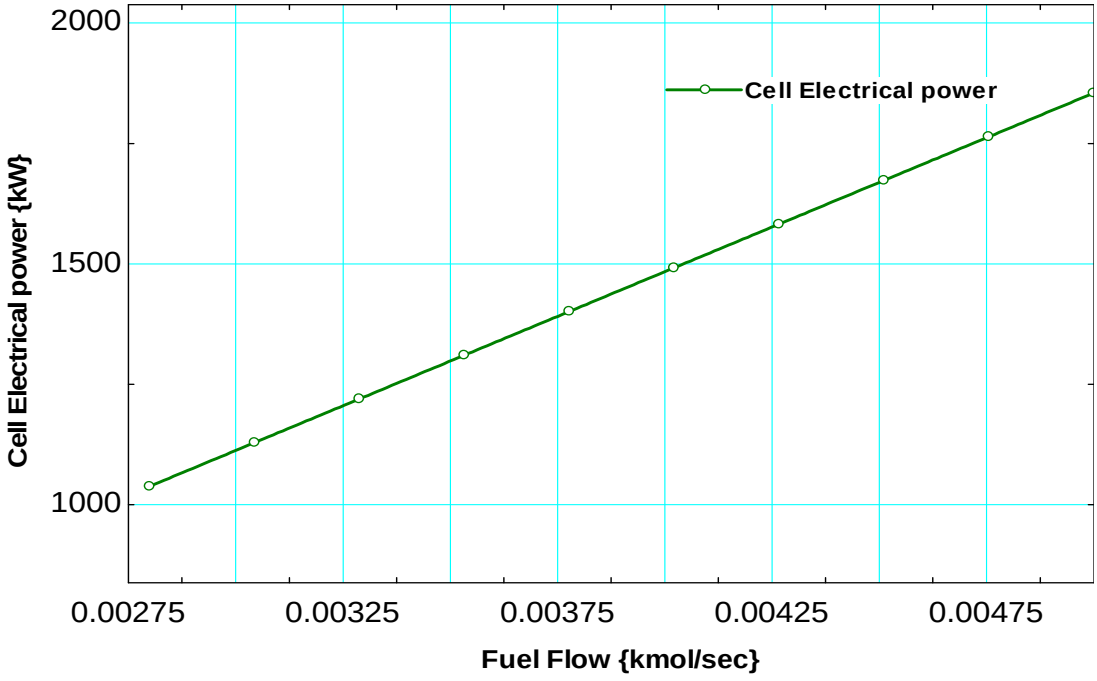

Figure 7.19: Cell work output vs. molar flow of fuel (Present model)

7.3.3 Effect of oxygen to carbon ratio

The oxygen to carbon ratio (OTCR) has a great impact on electrical efficiency of the combined hybrid system.

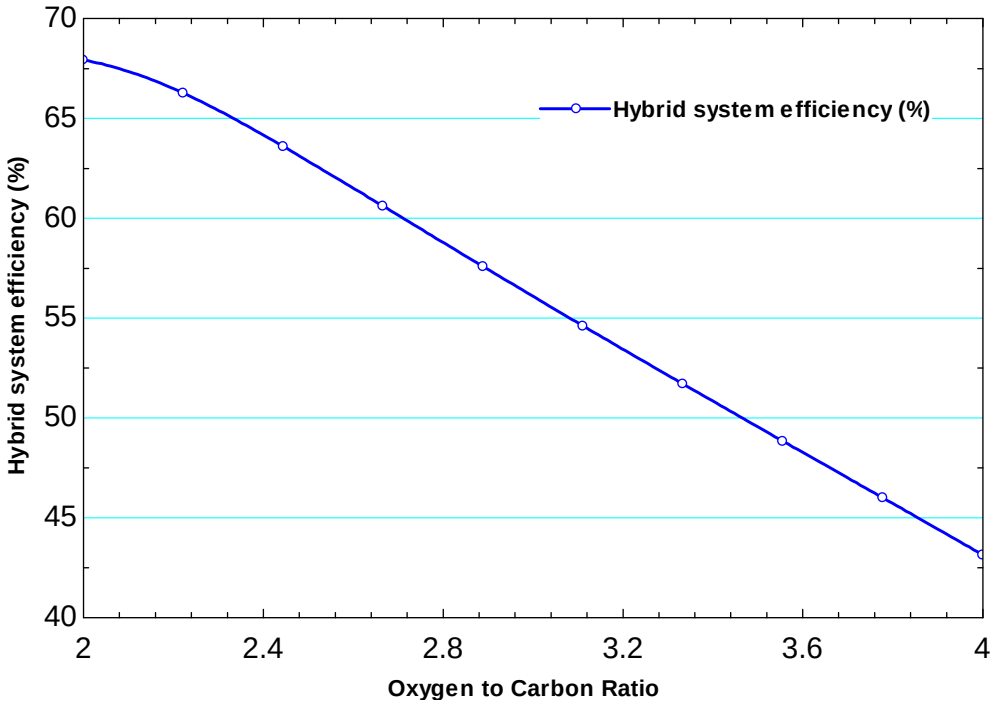

Figure 7.20: Hybrid system electrical efficiency vs. oxygen to carbon ratio (Present model)

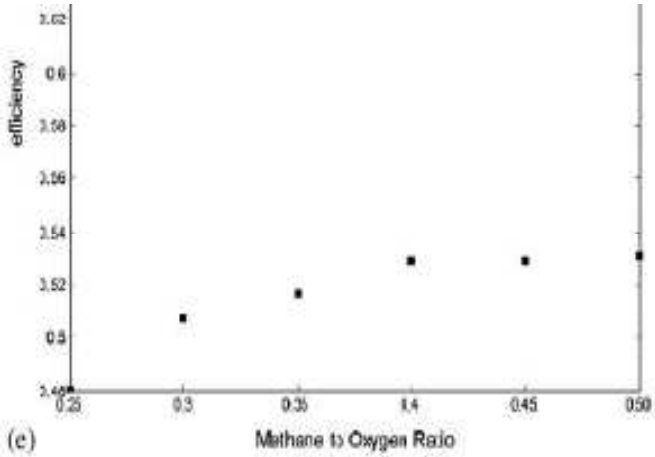

Figure 7.21: Hybrid system electrical efficiency vs. carbon ratio to oxygen (Literature) [48]

This is shown in Fig. 7.20, oxygen to carbon ratio has varied between 2 to 4 and corresponding to these values the electrical efficiency decreases from around 0.67 to 0.44. The oxygen to carbon ratio helps to provide a complete combustion in combustion chamber, but on another hand increases the compressor work due to increase in mass of air, and secondly higher oxygen results in decrease of operating temperature of the system with a constant fuel flow and increasing flow of oxygen in air.

7.3.4 Effect of fuel utilization efficiency

Another key parameter is the fuel utilization efficiency. Its effect on electrical efficiency of the SOFC/GT hybrid system is shown in Fig. 7.22. The efficiency increases with an increase in fuel utilization efficiency.

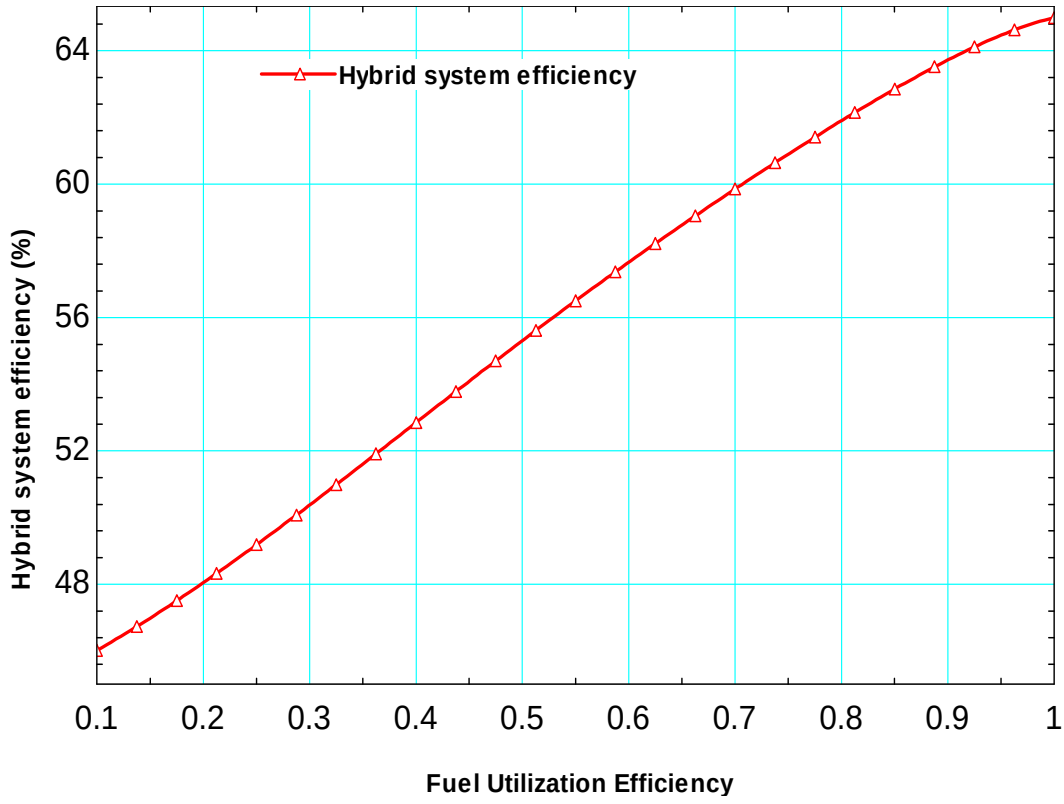

Figure 7.22: Hybrid system efficiency vs. Fuel utilization efficiency (Present model)

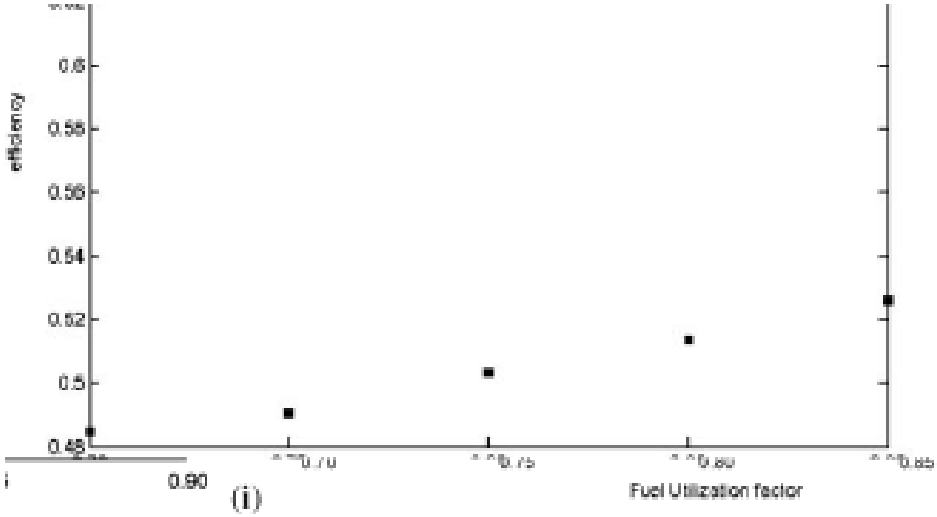

Figure 7.23: Hybrid system efficiency vs. Fuel utilization efficiency (Literature) [48]

7.3.5 Effect of steam to carbon Ratio

By varying the steam to carbon ratio (STCR) the system efficiency increases up to an optimum value of steam to carbon ratio.

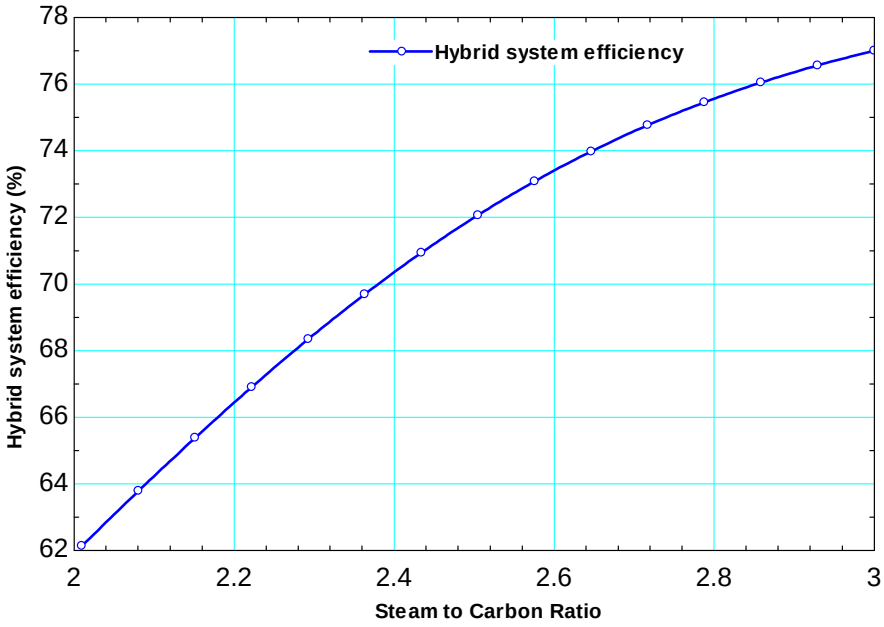

Figure 7.24: Hybrid system efficiency vs. Steam to carbon ratio (Present model)

Since up to a certain increase it promotes reforming reaction and after a particular limit it has no significant effect on the electrical efficiency of the system. For a variation of steam to carbon ratio from 2 to 3, a dramatic increase of efficiency is noticeable between the values 2 to 2.8.

7.3.6 Effect of cell operating temperature

By keeping other parameters constant, the effect of cell operating temperature on electrical efficiency of hybrid system and power output from SOFC unit and gas turbine unit has been studied and it is shown with the help of Fig. 7.25 and 7.26.

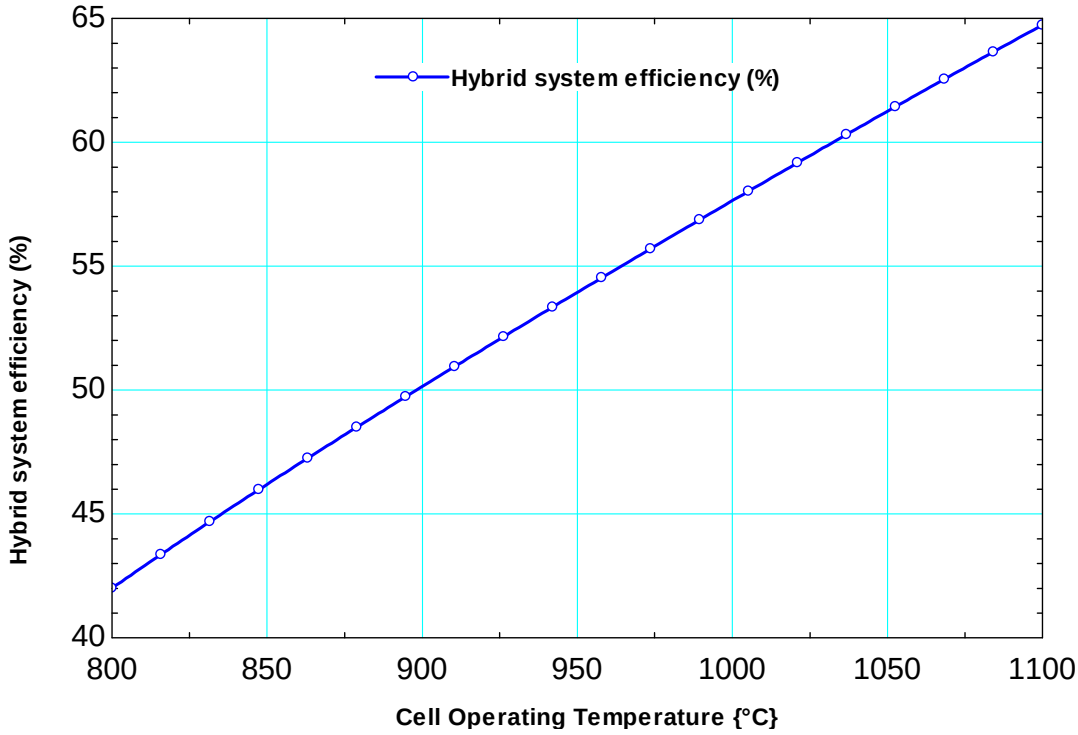

Figure 7.25: Electrical efficiency vs. Cell operating temperature (Present model)

The system efficiency is greatly influenced by the decrease in the cell operating temperature, decreasing temperature from 1100 to 800 ℃ results in decrease off electrical efficiency from 65% to 43%. Both the cell power output and gas turbine power increases with the increase in cell operating temperature, But the effect of cell operating temperature on cell power output is more as compared to its effect on gas turbine power output.

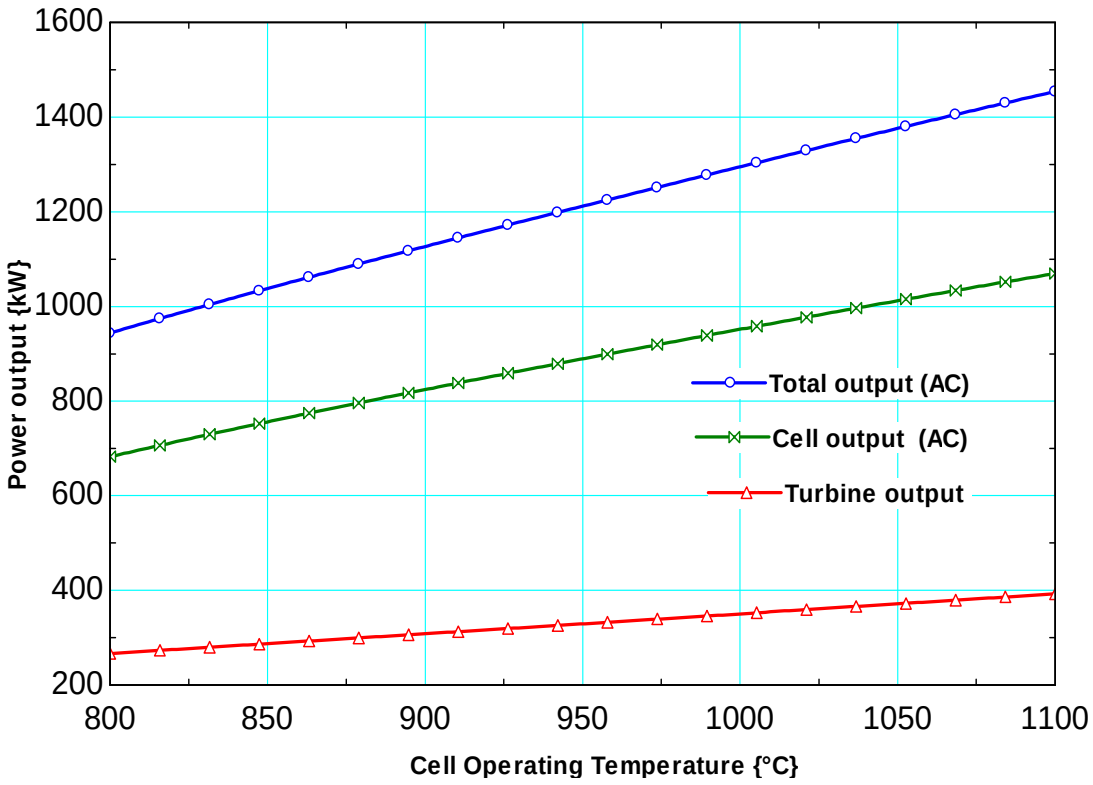

Figure 7.26: Power output vs. Cell operating temperature (Present model)

7.3.7 Effect of pressure ratio

Pressure ratio supplied here is the ratio of pressure at compressor inlet to pressure at compressor outlet which determines the cell operating pressure and the pressure at the inlet of turbine. The variation of the influence of pressure ratio on electrical efficiency of the combined system, power output of SOFC and turbine, and cell voltage is shown in Figure 7.27, 7.29, 7.28 and 7.30 respectively. It is reported that with increase in pressure ratio the electrical efficiency increases and approximately a linear relation is followed by the efficiency increase. From the Fig. 6.17 it is clear that hybrid system offers efficiency around 57% even at a very low pressure ratio of 4. The cell power output is also affected by the increase in pressure ratio, because as pressure ratio increases the cell operating pressure also increases. The effect of pressure ratio on turbine output is much more as compared to the cell power output, this is because as the pressure ratio increases the work consumed by the compressor also increases which is supplied by the gas turbine.

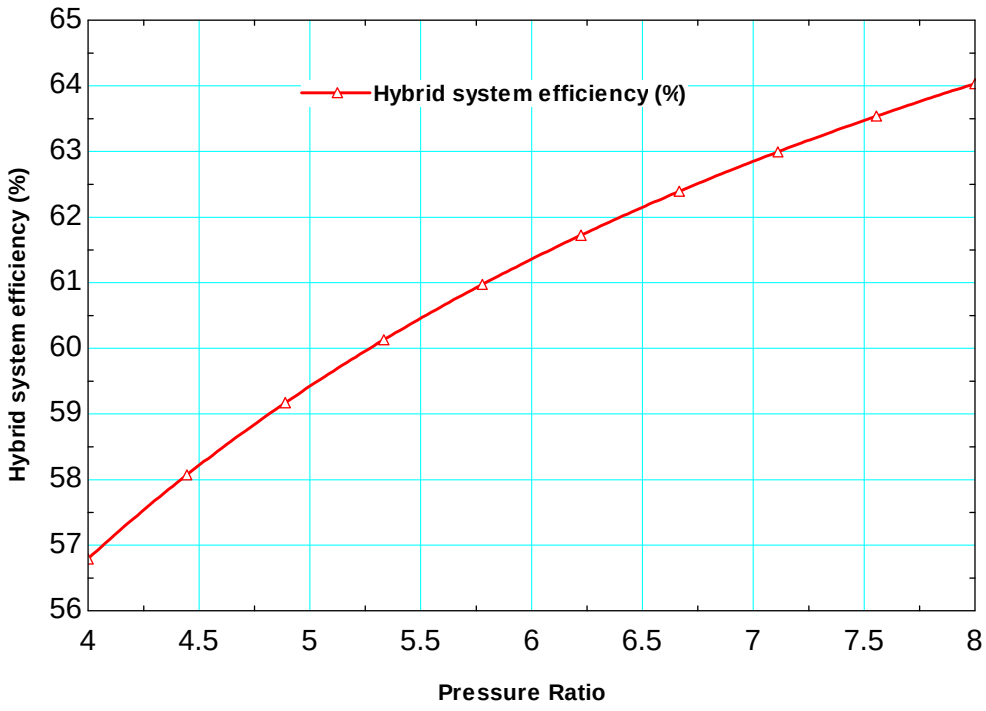

Figure 7. 27: Hybrid system efficiency vs. pressure ratio (Present model)

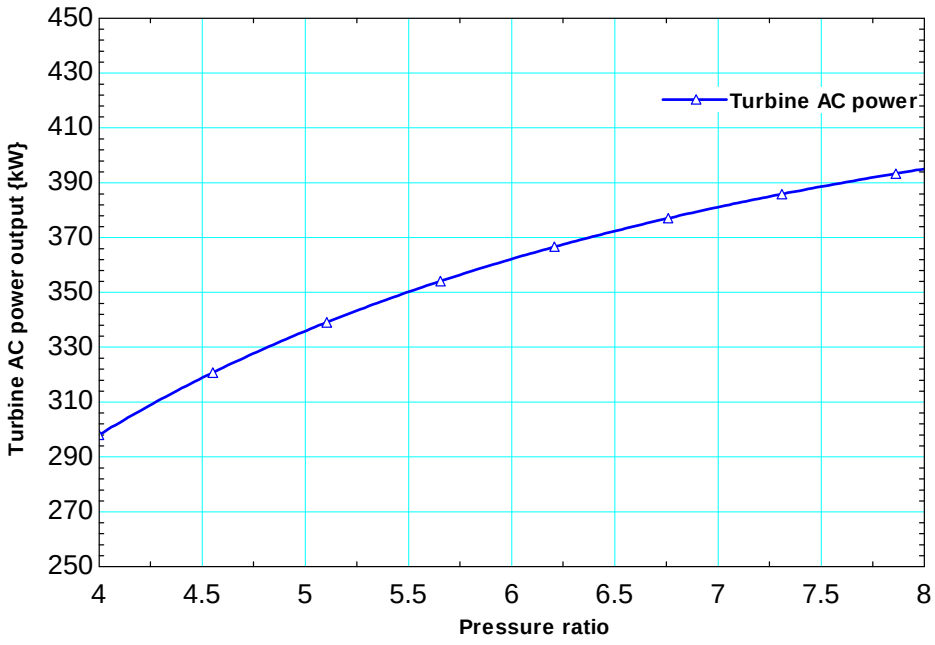

Figure 7.28: Turbine power output vs. Pressure ratio (Present model)

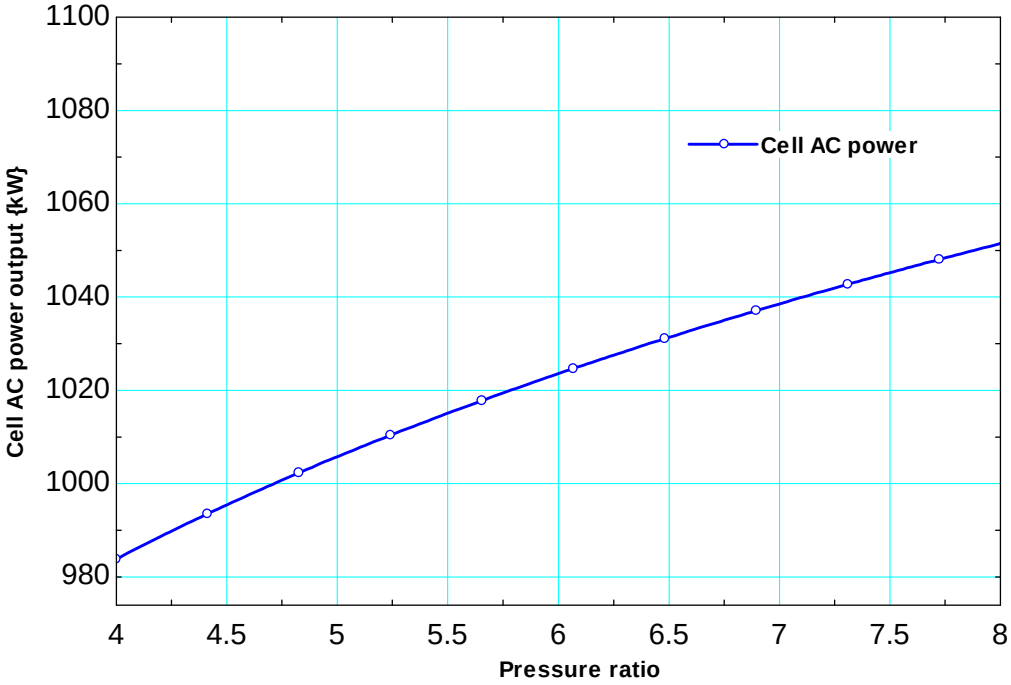

Figure 7.29: Cell power output vs. Pressure ratio (Present model)

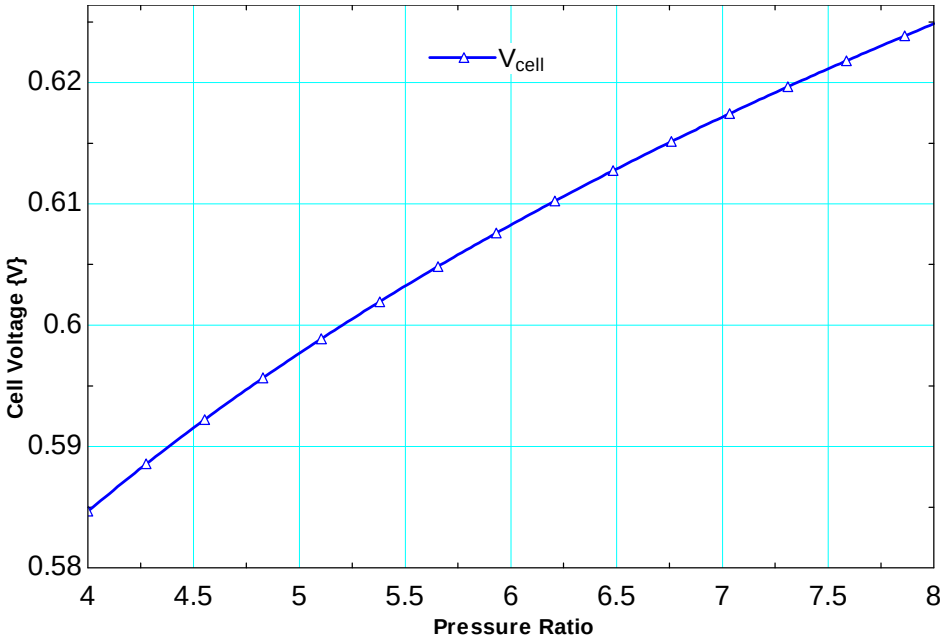

Figure 7.30: Cell voltage vs. Pressure ratio (Present model)

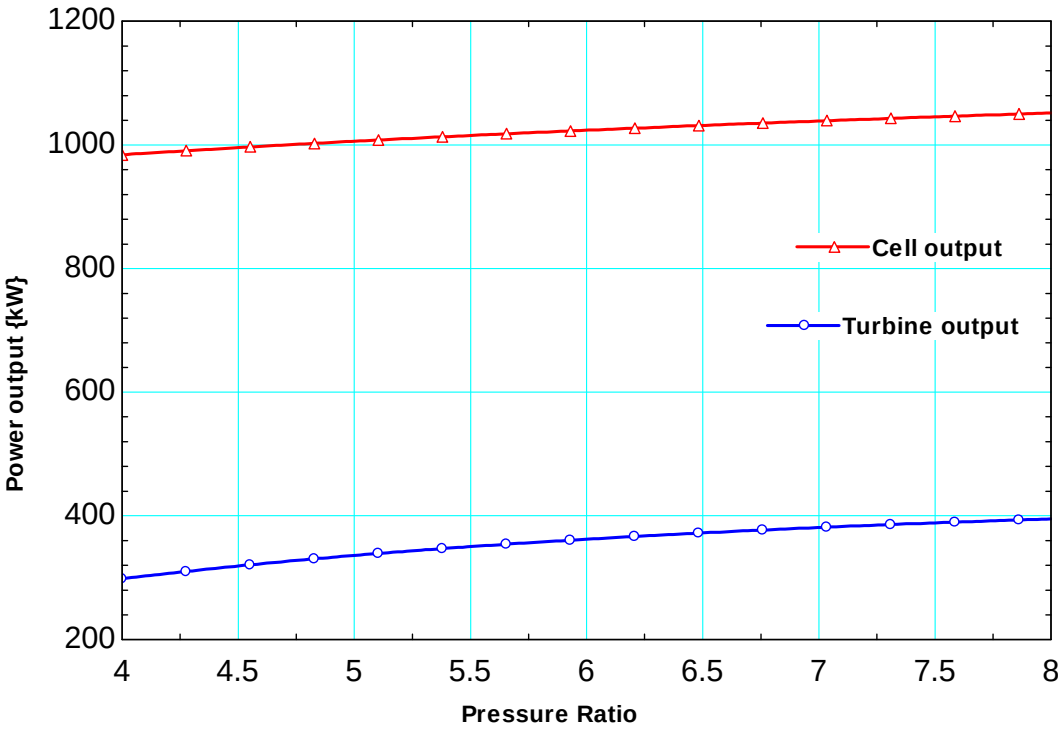

Figure 7.31: Power output vs. Pressure ratio (Present model)

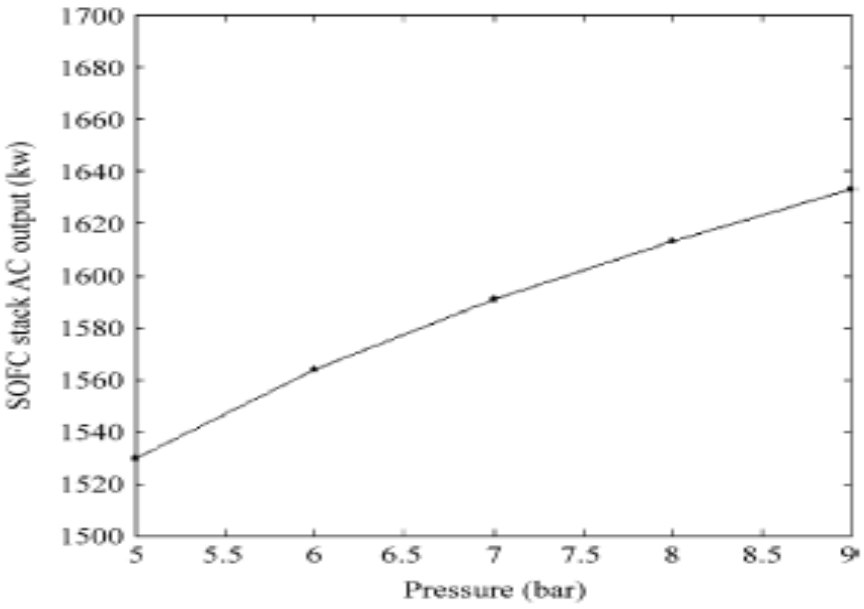

Figure 7.32: Cell power output vs. Pressure ratio (Literature) [41]

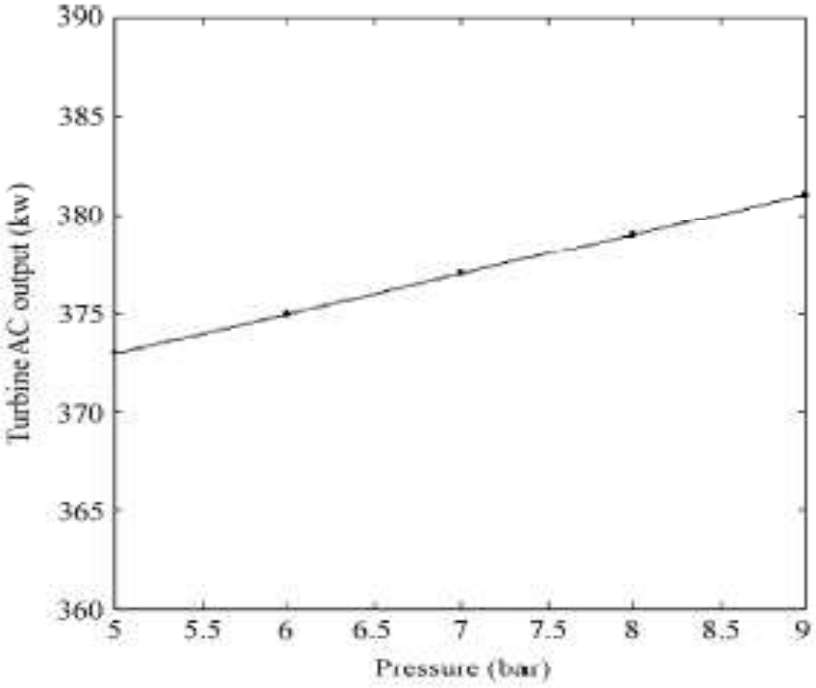

Figure 7.33: Turbine power output vs. Pressure ratio (Literature) [41]

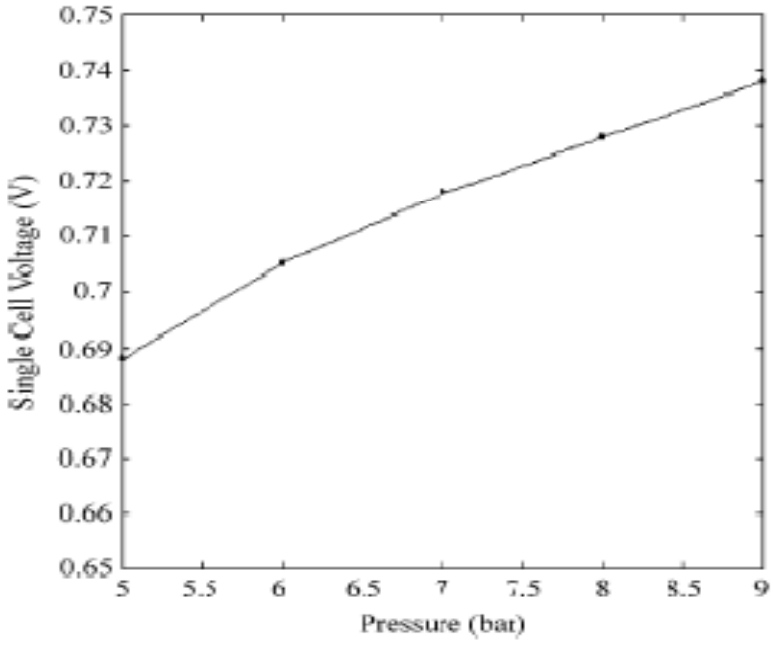

Figure 7.34: Cell voltage vs. Pressure ratio (Literature) [41]

Chapter 8

Conclusion and Future work

8.1 Conclusion

[1] A general-purpose design methodology has been developed for parametric study and performance evaluation of a gas turbine and solid oxide fuel cell hybrid system.

[2] The electrical efficiency based upon LHV of fuel is calculated and matched with literature. The efficiency reported by the simulation is in good agreement with the value of efficiency reported in the literatures.

[3] The cell voltage based upon constant limiting current density is calculated and matched with various literatures.

[4] Exergy at various state points of the system is calculated.

[5] Results obtained are validated with available literature.

[6] Based upon the input parameter supplied, developed model simulation calculated:
Cell voltage = 0.67 V,
Hybrid system first law electrical efficiency = 66.5 %.
Hybrid system second law efficiency = 63.5 %.

8.2 Recommendations for Future Work

The present work can be extended in following areas:

[1] Analysis can be extended for some more fuel cell geometries.

[2] The system can be easily extended for mixture of gases (such as syngas).

[3] Instead of constant limiting current density, its calculated value can be used.

[4] The present work can be extended for modeling of fuel cells for different polarization models available.

[5] The present work can be extended for the waste heat recovery available at system exhaust.

[6] The system can be extended for thermo economic analysis.

Table A. 1: Resistivity constants [58]

Component	a	b
Anode	0.0000298	-1392
Cathode	0.0000811	600
Electrolyte	0.0000294	10350
Interconnector	0.001256	4690

Table A. 2: Fuller Diffusion volume's

Gas Species	Fuller Diffusion vol. (v)
H_2	7.07
H_2O	12.7
O_2	16.6
N_2	17.9

Table B. 1: Demonstrations Summary of Fuel Cell and SOFC/GT Power Plants [3]

Year	Customer	Stack Rating (kWe)	Cell Length (mm)	No. of Cells/Stack	Oper. (Hrs)	Fuel
2006	BP Alaska	125	1500	1140	---------	PNG
2005	SW Hannover	125	1500	1140	---------	PNG
2002	OPT	250	1500	2304	1000+	PNG
2001	RWE	125	1500	1152	3872	PNG
2000	SCE PSOFC/GT	180	1500	1152	3257	PNG
1999	EDB/ELSAM-2	125	1500	1152	12,577	PNG
1998 S	CE-2/NFCRC	27	500	576	5700+	PNG
1997	EDB/ELSAM-1	125	1500	1152	4035	PNG
1995	JGU-2	25	500	576	13194	PNG
1995	SCE-2	27	500	576	5582	PNG DF-2 JP8
1994	SCE-1	20	500	576	6015	PNG
1993	Utilities-B2	20	500	576	7064	PNG
1992	Utilities-B1	20	500	576	1579	PNG
1992	Utilities-A	20	500	576	2601	PNG
1992	JGU-1	20	500	576	817	PNG
1987	Tokyo Gas	3	360	144	4882	H2+CO
1987	Osaka Gas	3	360	144	3683	H2+CO
1987	Osaka Gas	3	360	144	3012	H2+CO
1986	TVA	0.4	360	24	1760	H2+CO

References

[1] Haji Shaker, *"Analytical Modelling of PEM Fuel Cell i-V Curve"*, Renewable Energy 36: 451-458, 2011.

[2] Eugene L. Keating, *"Applied Combustion"*, CRC Press, 2nd Edition: 2007.

[3] www.siemens.com Global Website accessed on 14-06-2011.

[4] Stefano Campanari Ph.D., *"Thermodynamic model and parametric analysis of a tubular SOFC module"*, Journal of Power Sources 92: 26-34, 2001.

[5] Marcos V. Moreira, Gisele E. da Silva, *"A practical model for evaluating the performance of proton exchange membrane fuel cells",* Renewable Energy 34: 1734-1741, 2009.

[6] Ananda Himansu, Joshua E. Freeh, Christopher J. Steffen, Jr., Robert T. Tornabene, Xiao-Yen J. Wang, *"Hybrid Solid Oxide Fuel Cell/Gas Turbine System Design for High Altitude Long Endurance Aerospace Missions",* NASA/TM - 2006-214328, FUELCELL 2006-97095, May 2006.

[7] M. Santin, A. Traverso, A. Massardo, *"Technological aspects of gas turbine and fuel cell hybrid systems for aircraft: a review",* THE AERONAUTICAL JOURNAL, AUGUST 2008, VOLUME 112, NO. 1134: 459-467, 2008.

[8] Maher A. R. Sadiq Al-Baghdadi, *"Modelling of proton exchange membrane fuel cell performance based on semi-empirical equations", Renewable* Energy 30: 1587-1599, 2005.

[9] Sadik Kakaç, Anchasa Pramuanjaroenkij, Xiang Yang Zhou, "A *review of numerical modeling of solid oxide fuel cells"*, International Association for Hydrogen Energy, Elsevier Ltd., 2006.

[10] Tsang-Dong Chung, Wen-Tang Hong, Yau-Pin Chyou, Dong-Di Yu, Kin-Fu Lin b, Chien-Hsiung Lee, "*Efficiency analysis of solid oxide fuel cell power plant systems"*, Applied Thermal Engineering 28: 933-941, 2008.

[11] Nico Hotz, Stephan M. Senn, Dimos Poulikakos, "*Exergy analysis of a solid oxide fuel cell micro power plant"*, *Journal* of Power Sources 158: 333-347, 2006.

[12] A. Bharadwaj, D. H. Archer, E. S. Rubin, *"Modelling the Performance of a Tubular Solid oxide Fuel Cell"*, Transactions of the ASME, vol. 2: 38-44, 2005.

[13]Wayne Doherty, Anthony Reynolds, David Kennedy, *"Modeling and simulation of a biomass Gasification-solid oxide fuel cell combined heat and power plant using Aspen Plus"*, In 22nd International Conference on Efficiency, Cost, Optimization Simulation and Environmental Impact of Energy Systems, Foz do Iguacu, Parana, Brazil August 31- September 3, 2009.

[14] Adam Hahn, *"Modeling and control of solid oxide fuel cell - gas turbine power plant systems",* Master Thesis, University of Pittsburgh, 2000.

[15] Yousef S.H. Najjar, *"Gas turbine cogeneration systems: a review of some novel cycles"*, Applied Thermal Engineering 20: 179-197, 2000.

[16] Yousef S. H. Najjar, *"Enhancement of performance of gas turbine engines by inlet air cooling and cogeneration system"*, Applied Thermal Engineering 16(2):163 - 173, 1996.

[17] Maria Jonssona, Jinyue Yan, *"Humidified gas turbines—a review of proposed and implemented cycles"*, Energy 30: 1013-1078, 2005.

[18] P.A. Pilavachi*, "Power generation with gas turbine systems and combined heat and power"*, Applied Thermal Engineering 20: 1421-1429, 2000.

[19] Santin Marco, Traverso Alberto, Magistri Loredana, *"Liquid fuel utilization in SOFC hybrid systems*", Applied Energy 86: 2204-2212: 2009.

[20] A. Salogni, P. Colonna, *"Modeling of solid oxide fuel cells for dynamic simulations of integrated systems",* Applied Thermal Engineering 30: 464–477, 2010.

[21] Denver F. Cheddie, Renique Murray, *"Thermo-economic modeling of an indirectly coupled solid oxide fuel cell/gas turbine hybrid power plant"*, Journal of Power Sources 195: 8134-8140, 2010.

[22] www.siemens.com Global Website accessed on 28-06-2011.

[23] Shinji Kimijima, Nobuhide Kasagi, *"Performance Evaluation of Gas Turbine-Fuel Cell Hybrid Micro Generation system"* , *ASME* TURBO EXPO 2002, June 3-6, Amsterdam, The Netherlands, 2002.

[24] Kartha Sivan, Kreutz Thomas G., Williams Robert H., "*Small-scale biomass fuel cell/gas turbine power systems for rural areas"*, Energy for Sustainable Development, Volume IV No. 1, June 2000.

[25] A. Sordi, E. P. da Silva, A. J. M. Neto, D. G. Lopes, C. S. Pinto, P. D. Araújo, *"THERMODYNAMIC SIMULATION OF BIOMASS GAS STEAM REFORMING FOR A SOLID OXIDE FUEL CELL (SOFC) SYSTEM",* Brazilian Journal of Chemical Engineering, Vol. 26, No. 04, pp. 745 - 755, October - December, 2009.

[26] Senthil V. Vannivedu Umapathi, Kiran Rao Bhimma, Parchuri M. V. Subbarao, *"Performance Analysis of Hybrid Solid Oxide Fuel Cell - Gas Turbine Power Generating System"*, The 2nd Joint International Conference on "Sustainable Energy and Environment (SEE 2006)", 21-23 November 2006, Bangkok, Thailand, 2006.

[27] Luigi Leto, Celidonio Dispenza, Angelo Moreno, Antonio Calabro, *"Simulation model of a molten carbonate fuel cell-microturbine hybrid system",* Applied Thermal Engineering xxx: 1-9, 2011.

[28] Rama S.R. Gorla, *"Probabilistic analysis of a solid-oxide fuel-cell based hybrid gas-turbine system",* Applied Energy 78: 63-74, 2004.

[29] Xiao-Juan Wu, Qi Huang, Xin-Jian Zhu, *"Thermal modeling of a solid oxide fuel cell and micro gas turbine hybrid power system based on modified LS-SVM"*, international journal o f hydrogen energy 36 :885 - 892, 2011.

[30] Said Al-Hallaj, Fuad Alasfour, Sandeep Parekh, Shabab Amiruddin, J. Robert Selman, Hossein Ghezel-Ayagh, *"Conceptual design of a novel hybrid fuel cell/desalination system",* ELSEVIER, Desalination 164: 19-31, 2004.

[31] C. Bang-Moller, M. Rokni, "*Thermodynamic performance study of biomass gasification, solid oxide fuel cell and micro gas turbine hybrid systems"*, Energy Conversion and Management 51: 2330 – 2339, 2010.

[32] Siemens, "*Pictures of the Future",* p. 98, Spring 2007.

[33] Y. Haseli, I. Dincer, G.F. Naterer, *"Thermodynamic modeling of a gas turbine cycle combined with a solid oxide fuel cell"*, International Journal of Hydrogen Energy 33: 5811-5822, 2008.

[34] S. P. Harvey, H.J. Richter, *"A detailed study of a gas turbine cycle with an integrated internal reforming solid oxide fuel cell"*, In Proceedings of 29th Intersociety energy conversion engineering conference, vol. 2: 961-973, Monterey, CA, 1994.

[35] S. P. Harvey, H. J. Richter, *"Gas turbine cycles with solid oxide fuel cells. Part II: A detailed study of a gas turbine cycle with an integrated internal reforming solid oxide fuel cell"*, Transactions of the ASME. J Energy Res Technol; 116(4): 312-318, 1994.

[36]K. Lobachyov, H. J. Richter, *"Combined cycle gas turbine power plant with coal gasification and solid oxide fuel cell",* Transactions of the ASME J. Energy Resour Technol 118(4): 285-292, 1996.

[37] R. A. George, *"SOFC combined cycle systems for distributed generation"*, In Proceedings of the American Power Conference, vol. 59-1: 548-550, Chicago, IL, 1997.

[38] S. Campanari, E. Macchi, *"Thermodynamic analysis of advanced power cycles based upon solid oxide fuel cells, gas turbines and rankine bottoming cycles"*, In Proceedings of the International gas turbine and aero engine congress and exhibition, Stockholm, 1998.

[39] J. Palsson, A. Selimovic, L. Sjunnesson, *"Combined solid oxide fuel cell and gas turbine systems for efficient power and heat generation"*, Journal of Power Sources 86(1–2): 442-448, 2000.

[40] P. Costamagna, L. Magistri, A. F. Massardo, "*Design and part-load performance of a hybrid system based on a solid oxide fuel cell reactor and a micro gas turbine"*, Journal of Power Sources 96: 352-368, 2001.

[41]S. H. Chan, H. K. Ho, Y. Tian , "*Modelling of simple hybrid solid oxide fuel cell and gas turbine power plant"*, Journal of Power Sources 109: 111-120, 2002.

[42] A. F. Massardo, C. F. McDonald, T. Korakianitis, "Microturbine/ fuel-cell coupling for high-efficiency electrical-power generation", Transactions of the ASME Journal of Eng Gas Turbines Power 124(1): 110-116, 2002.

[43]A. D. Rao, G. S. Samuelsen, *"A thermodynamic analysis of tubular solid oxide fuel cell based hybrid systems"* ,Transactions of the ASME Journal of Eng Gas Turbines Power 125(1):59-66, 2003.

[44] S. H. Chan, H. K. Ho, Y. Tian , "Mu*lti-level modeling of SOFC–gas turbine hybrid system"*, International Journal of Hydrogen Energy 28: 889-900, 2003.

[45] Y. Inui, S. Yanagisawa, T.Ishida, "*Proposal of high performance SOFC combined power generation system with carbon dioxide recovery"*, Energy Conversion Management 44(4):597-609, 2003.

[46] H. Uechi, S. H. Kimijima, N. Kasagi, *"Cycle analysis of gas turbine-fuel cell cycle hybrid micro generation system"*, Journal of Eng Gas Turbines Power 126(4):755-762, 2004.

[47] F. Calise, A. Palombo, L. Vanoli, *"Design and partial load exergy analysis of hybrid SOFC–GT power plant"*, Journal of Power Sources 158(1):225-244, 2006.

[48]F. Calise, M. Dentice d'Accadia,A. Palombo, L.Vanoli, "*Simulation and exergy analysis of a hybrid solid oxide fuel cell (SOFC)–gas turbine system"*, Energy 31: 3278-3299, 2006.

[49] T. Araki, T. Ohba, S. H. Takezawa, K. Onda, Y. Sakaki, "Cycle *analysis of planar SOFC power generation with serial connection of low and high temperature SOFCs"*, Journal of Power Sources 158(1): 52-59, 2006.

[50] T. Araki, T. Taniuchi, D. Sunakawa, M. Nagahama, K. Onda, T. Kato, *"Cycle analysis of low and high H2 utilization SOFC/ gas turbine combined cycle for CO2 recovery"*, Journal of Power Sources 171(2):464–470, 2007.

[51] L. Tse, F. Galinaud, R. F. Martinez-Botas, *" Integration of solid oxide fuel cells into a gas turbine cycle"*, ASME turbo expo power for land, Sea and Air, http://www.felicitas-fuel-cells.info/files/061101_ASME2007_Tse.pdf Pala is Des Congres Montreal DRAFT, 2007.

[52] Dieter Bohn, *"Micro Gas Turbine and Fuel Cell – A Hybrid Energy Conversion System with High Potential"*, In Micro Gas Turbines Educational Notes RTO-EN-AVT-131, Paper 13: 13.1-13.46 Neuilly-sur-Seine, France: 2005.

[53] Department of Energy U.S. "Fuel Cell Handbook" U.S. Department of Energy, Office of Fossil Energy, National Energy Technology Laboratory, 5th Edition: 2000.

[54] Jeongpill Ki, Daejong Kim, *"Computational model to predict thermal dynamics of planar solid oxide fuel cell stack during start-up process"*, Journal of Power Sources 195: 3186-3200, 2010.

[55] D. Mogensen, J.-D. Grunwaldt, P.V. Hendriksen, K. Dam-Johansen, J.U. Nielsen, *"Internal steam reforming in solid oxide fuel cells: Status and opportunities of kinetic studies and their impact on modelling",* Journal of Power Sources 196: 25-38, 2011.

[56] Mathew M. Mench, *"Fuel Cell Engines"*, John Wiley & Sons, 2008.

[57] J. Tafel, Z., "*Physik. Chem*.", Vol. 50A, p. 641, 1905.

[58] Sadegh Motahar, Ali Akbar Alemrajabi, *"Exergy based performance analysis of a solid oxide fuel cell and steam injected gas turbine hybrid power system"*, International Journal of Hydrogen Energy 34: 2396-2407, 2009.

[59] Scott Samuelsen, *"Fuel Cell/Gas Turbine Hybrid Systems"*, ASME International Gas Turbine Institute, 2004.

[60] A. Bejan, M. J. Moran, "Thermal System Design and Optimization", John Wiley & Sons, 1996.

[61] S.H. Chan, K.A. Khor, Z.T. Xia, "*A complete polarization model of a solid oxide fuel cell and its sensitivity to the change of cell component thicknes"*, Journal of Power Sources 93 :130 – 140, 2001.